On Relay-assisted Cellular Networks

A thesis submitted in partial fulfillment of
the requirements for the degree of

Bachelor of Technology
in *Electrical Engineering*
&
Master of Technology
in *Communications and Signal Processing*

(under the Dual Degree Programme)

by

Gauri Joshi
(Roll No. 05D10019)

Under the guidance of
Prof. Abhay Karandikar

Department of Electrical Engineering
INDIAN INSTITUTE OF TECHNOLOGY–BOMBAY
June, 2010

Dissertation Approval

This dissertation entitled *On Relay-assisted Cellular Networks* by
Gauri Joshi is approved for the degrees of Bachelor of Technology in Electrical Engineering
and Master of Technology in Communication and Signal Processing.

Internal Examiner : _____

Additional Internal Examiner : _____

Supervisor : _____

Chairman : _____

23rd June 2010
IIT Bombay

Declaration

I declare that this written submission represents my ideas in my own words and where others' ideas or words have been included, I have adequately cited and referenced the original sources. I also declare that I have adhered to all principles of academic honesty and integrity and have not misrepresented or fabricated or falsified any idea/data/fact/source in my submission. I understand that any violation of the above will be cause for disciplinary action by the Institute and can also evoke penal action from the sources which have thus not been properly cited or from whom proper permission has not been taken when needed.

Gauri Joshi

05D10019

23rd June 2010

To my parents

Acknowledgments

Date: _____   Gauri Joshi

Abstract

Cellular operators are developing low-cost relays to improve the coverage and capacity of next generation cellular networks. Deploying low cost relays reduces the infrastructure cost of setting up new base stations in order to support the rapidly growing number of subscribers. In this thesis, we present methods to design the system architecture and efficient protocols to achieve maximum benefit from the introduction of cellular relays. We focus on three of these issues- relay placement for coverage extension, capacity improvement with relays and relay automatic repeat request (ARQ) protocols.

The first problem considered is relay placement for maximum extension of the cell radius. Increase in cell radius helps reduce infrastructure cost of deploying more base stations to support the rapidly growing number of subscribers. We define the notion effective radius of the cell in terms of the probability of correct decoding at a point, and determine the optimal relay position which maximizes the effective cell radius. We also analyze the multicell scenario, by taking into account inter-cell interference and present an iterative algorithm to determine the relay positions.

Apart from coverage extension, cellular relays also improve the cell capacity. This is because mobile stations get the advantage of diversity due to two possible signal paths - one directly from the base station, and another via a relay. Thus, incoming calls experience lower blocking probability. We present a novel approach to determine the downlink Erlang capacity of the cell. Then, we extend this idea to evaluate the Erlang capacity for relay-assisted cellular networks, and demonstrate how a capacity improvement takes place.

Lastly, we analysis ARQ protocols for relay-assisted cellular networks. We demonstrate that major packet loss takes place during handover in the hop-by-hop ARQ protocol. We present a novel channel and handover model and use it to quantify this packet loss. Then, we propose modifications to hop-by-hop ARQ which reduce the packet loss during handover, at the cost of an increase in queueing delay. Time delay analysis is performed to show that the increase in queueing delay is negligible.

Contents

List of Figures

Chapter 1

Introduction

With a rapid growth of the number of cellular subscribers, and the scarcity of frequency spectrum, cellular systems are facing difficulty in providing satisfactory signal to noise ratio (SNR) to users, especially to those at the cell edge. One solution to support the increasing number of subscribers per cell is to decrease the cell radius. This results in a greater number of base stations required per area thus escalating the infrastructure costs. Also, smaller cell radius causes higher inter-cell interference, thereby calling for better frequency planning techniques such as sectorization to minimize interference.

An alternate solution being employed in next generation cellular systems [1, 2] is to deploy low-cost cellular relay stations (RSs) in each cell to improve the system capacity and coverage area. A relay station (RS) is a node which assists in the transmission of data between other nodes in the network. It may be a dedicated RS, whose purpose is solely to forward data for other nodes, or a cooperative relay which assists other nodes when it does not have packets for transmission in its own queue. In this chapter, we give a brief overview of relays and their applications to wireless cellular networks.

1.1   Types of Relays

RSs can be broadly classified into the two types- amplify-and-forward RSs and decode-and-forward RSs. An amplify-and-forward RS receives the signal and simply amplifies it before transmitting the copy. Since the signal is not decoded, the signal quality is degraded. Amplify-and-forward RSs are low complexity and easy to implement. A decode-and-forward RS decodes the received signal and re-encodes it before forwarding a copy.

Due to decoding, the noise in the received signal is cleaned out. Because of the presence of decoder and encoder, decode-and-forward relays are of high complexity.

For application of relays to cellular systems, the IEEE 802.16m WiMAX standard [1, 2] has given preference to decode-and-forward RSs over amplify-and-forward RSs. We concentrate on decode-and-forward relays in the rest of this thesis. In the cellular scenario, decode-and-forward relays have been further classified into the following two categories:

- **Transparent relays:** Transparent RSs do not communicate any control signals to the mobile station (MS). The MS is essentially unaware of the presence of these RSs. In the uplink, they merely overhear the MS's transmission to the base station (BS) and forward a decoded and re-encoded copy to the BS when requested to do so. Since the MS does not exchange control signals with the RS, it performs power control according to the uplink channel to the BS, and not to the RS. Thus, introduction of transparent RSs does not help in saving the MS's uplink transmit power. However, if the BS-MS channel is in a deep fade, the RSs provide spatial diversity and improve network coverage to these MSs.

- **Non-transparent relays:** Non-transparent RSs can transmit control signals to the MS. They can perform most of the functions of a full-fledged base station. When an MS moves away from the BS and close to an RS, it is handed over to the RS by a procedure similar to an inter-BS handover. The major difference between an RS and a full-fledged BS is that the RS is not directly connected to the backhaul network. Since a non-transparent RS transmits pilot signals to the MS, for uplink transmissions, the MS will just transmit enough power to reach the RS. This will result in significant power saving at the MS in addition to better network coverage. The IEEE 802.16m WiMAX standard [1, 2] currently supports non-transparent RSs over transparent RSs. In the rest of the thesis, we consider decode and forward, non-transparent cellular RSs.

1.2 Improvement in cellular networks due to relays

Relays are introduced in cellular networks to achieve improvement in the following aspects:

- **Coverage:** RSs improve the network coverage to MSs, especially at the cell edge.

A cell edge MS may experience poor received SNR from the BS, but being closer to the RS, the MS receives a strong signal from the RS with high probability. Thus, introduction of RSs increases the total coverage area of the cell, [3, 4]. By increasing the cell radius the number of base stations would decrease. If the total cost of RSs is less than that of this decrease in the base stations, the infrastructure cost would reduce to a great extent.

- **Capacity:** Alternative to increasing the coverage area, RSs can be used to increase the capacity of the cell. Because of the improvement in signal quality experienced by users at the cell edge, these users require lesser resources from the BS. For example, in cellular OFDMA systems, the number of subcarriers required by the user is smaller when the MS is served via an RS. Thus, the same resources can be shared among a larger number of users resulting in overall capacity improvement.

1.3   Motivation for the thesis

Relays have been studied extensively for mesh and ad-hoc wireless networks [5]. However, it is only recently that RSs are finding application for improving the capacity and coverage in cellular networks [6]. The main difference between RSs for ad-hoc networks and cellular RSs is that unlike ad-hoc RSs, the currently proposed cellular RSs do not communicate with each other directly. They exchange information only via the BS. Due to limited frequency spectrum in cellular systems, this communication between RS and BS has to be minimized while ensuring high system performance.

Another feature of relay-assisted cellular networks which differs from ad-hoc networks is that an MS is handed over to a cellular RS using a procedure similar to inter-BS handover. In the currently proposed architecture, there is no cooperative combining of packets being received at the MS via different paths (directly from BS, or via one or more RS). Finally, unlike ad-hoc networks where there may be a large number of RSs between the source and destination, in practical cellular networks there are very few RSs (1 2) in a path from the BS to MS.

Due to these fundamental differences between ad-hoc and cellular networks, the traditional multihop protocols such as automatic-repeat-request (ARQ) which have been well studied for ad-hoc multihop networks, need to be modified in order to adapt to the

cellular scenario. The aim of this thesis is to address such issues and design an efficient architecture for relay-assisted cellular networks. In particular, we address issues such as optimal RS placement for cellular coverage extension, system capacity improvement with RSs, and modifications to traditional multihop ARQ protocols to reduce packet loss during handover.

1.4   Organization

In this chapter, we have discussed the basic concepts of RS and the advantages of introducing RSs in cellular networks. The rest of the thesis is organized as follows. Chapter 2 identifies the open research issues in relay-assisted cellular networks and summarizes our contributions towards solving some of these research problems. Chapter 3 presents an analysis of optimal relay placement in cellular networks. Chapter 4 presents a novel method for evaluation of the Erlang capacity of cellular OFDMA with and without RSs. Chapter 5 analyzes packet loss during handover in various ARQ protocols and proposes new protocols to reduce the packet loss. Finally, Chapter 6 concludes the thesis and provides directions for future work.

Chapter 2

Some Research Issues

In this chapter we formulate some open research issues for relay-assisted for cellular networks. We also discuss our contributions to the problems which have been addressed in the subsequent chapters.

2.1 Optimal Relay placement for Coverage Extension

The deployment of RS in cellular networks helps improve the system capacity and coverage area. In a relay-assisted cellular system, mobile stations (MSs) have the diversity benefit of two possible links, the direct link to the BS, and a link via RS. Thus, incoming calls experience lower blocking probability and the call can support a higher traffic load of users. The introduction of RSs also helps increase coverage radius of the cell by providing high SNR to the cell edge MSs. Thus, the infrastructure cost of deploying more base stations is reduced. In this work, we concentrate on the role of RSs in cellular coverage extension.

The increase in coverage radius of the cell depends upon the placement of RSs in the cell. This is because the location of RSs affects the quality of the BS-RS and RS-MS links as well as the inter-cell interference from neighboring cells. If an RS is placed too close to the cell edge, packets will experience a low SNR on the BS-RS link. Also, an RS close to the cell edge will cause higher interference to the neighboring cells. On the other hand, if the RS is placed close to the base station, the RS-MS link quality will suffer and cell edge users shall not benefit from the introduction of RSs. Thus for a given set of system parameters, there is a need for optimal RS placement to achieve maximum extension of

the coverage radius of the cell.

Only a few researchers so far have addressed the issue of optimal placement of cellular RSs. The authors in [7] and [8] analyze RS placement for wireless sensor networks, where the objective is to achieve maximum connectivity between pairs of ad-hoc relay nodes. In [9] and [10], the RS placement problem is analyzed from the perspective of increasing system capacity rather than coverage radius extension. [11] considers a dual-relay architecture with cooperative RS pairs and proposes an algorithm to select the two best RS locations from a predefined set of candidate positions. In [12], an iterative RS placement algorithm is proposed which divides all points in the cell into good and bad coverage points and places RSs at the good points whose neighbors have bad coverage. However, factors like shadowing and inter-cell interference have not been considered in the aforementioned papers. We perform a probabilistic analysis to compute optimal RS positions by taking account the random variables such as shadowing and inter-cell interference.

In Chapter 3, we analyze RS placement in cellular networks for extension of the cellular coverage area. Unlike existing literature, our treatment of optimal RS placement takes into account shadow fading and inter-cell interference. We present a novel probabilistic definition of coverage and evaluate the effective cell radius of the cell in terms of the required probability of coverage at the cell edge. We determine the optimal position of the RSs for which effective cell radius is maximized, and also obtain an estimate of the number of RSs required in each cell. Considering inter-cell interference from neighboring cells in the multicell scenario, leads to an interesting iterative optimization algorithm which is used to determine the optimal RS positions.

2.2   Capacity Improvement with Relays

Recent years have witnessed the emergence of Orthogonal Frequency Division Multiple Access (OFDMA) as one of the dominant Medium Access Control (MAC) techniques for next-generation wireless networks [2]. OFDMA employs multicarrier modulation to combat frequency selective fading. Each base station (BS) has a set of orthogonal subcarriers, subsets of which are allocated to users in the cell. Due to limited availability of spectrum, a 1:1 frequency reuse factor is most common in multi-cell OFDMA architecture. In 1:1

reuse, by allocating a random permutation of subcarriers to users in each cell, the inter-cell interference may be averaged out and hence may not affect the system performance severely.

Erlang capacity corresponds to the traffic load that a cell can support while providing acceptable service to the users. It is an important parameter from the capacity planning perspective and is used as a performance metric for admission control algorithms. In this chapter, we determine the downlink Erlang capacity of cellular OFDMA. The main idea is to take into account the fact that each incoming user requires a random number of subcarriers depending upon its position in the cell, fading and inter-cell interference.

Erlang capacity is a well studied topic for the traditional Global System for Mobile communications (GSM) cellular systems [13]. The capacity of these systems for a given blocking probability is determined by the Erlang-B formula. Erlang capacity has also been studied extensively in the context of Code Division Multiple Access (CDMA) systems [14, 15, 16]. Unlike GSM in which a user is blocked if all the time or frequency channels at the BS are occupied, in CDMA, an incoming user is blocked if it increases the interference and causes outage conditions for the existing users.

Though OFDMA is also a form of Frequency Division Multiple Access (FDMA), the fundamental difference between Erlang capacity of FDMA systems and cellular OFDMA is that in the latter, each call requires a random number of subcarriers. The idea of incoming users requiring random number of resources has been addressed in operations research literature [17]. A queueing system with Poisson arrivals of customers and exponentially distributed service times has been analyzed and the probability distribution of the waiting times of customers has been determined in [17].

Only a few studies focus on determining the Erlang capacity of cellular OFDMA [18, 19]. In [18], Erlang capacity is used as a performance metric for comparison of various adaptive resource allocation algorithms. In [19], the uplink capacity of relay-assisted cellular networks is analyzed. The authors present a joint algorithm to determine the bandwidth distribution between BS and RSs and the Erlang capacity for given values of blocking and outage probabilities. However, in both these papers, the random subcarrier requirement of a user is not considered in the derivation of blocking probability.

In Chapter 4, we present a novel approach to evaluate the downlink Erlang capacity of a cellular Orthogonal Frequency Division Multiple Access (OFDMA) system with 1:1

frequency reuse. Erlang capacity analysis of traditional cellular systems like Global System for Mobile communications (GSM) cannot be applied to cellular OFDMA because in the latter, each incoming call requires a random number of subcarriers. To address this problem, we determine the probability distribution of the number of subcarriers required, and divide incoming calls into classes according to their subcarrier requirement. We model the system as a multi-dimensional Markov chain and evaluate the blocking probability and Erlang capacity of the system. We draw an interesting analogy between the problem considered and the concept of a stochastic knapsack, a generalization of the classical knapsack problem. Techniques used to solve the stochastic knapsack problem simplify the analysis of the multi-dimensional Markov chain. We extend this analysis to relay-assisted cellular networks and determine the capacity increase of the system with introduction of RSs. We also compute the optimal BS-RS subcarrier distribution and the positions of RSs to maximize the system capacity.

2.3   Relay Automatic Repeat Request (ARQ)

For reliable transmission in multi-hop cellular networks, Automatic Repeat reQuest (ARQ) protocol is usually employed for the retransmission of erroneously received packets. End-to-end and hop-by-hop ARQ are the traditionally implemented multi-hop ARQ protocols.

In the end-to-end ARQ protocol, the RS merely forwards the data and ACK/NACK packets between the BS and the MS. The packet retransmissions are performed by the BS. This protocol ensures end-to-end reliability of the packet transmission, but the retransmission of packets by the BS leads to very low throughput performance as compared to protocols in which RS performs the retransmissions. Also, due to the high transmission error rate on the RS-MS link, the ACK/NACK from the MS to the BS may be delayed. Another disadvantage is that the power of a strong BS-RS link is not utilized by the end-to-end ARQ protocol. The BS schedules packets for transmission based on the ACK/NACK feedback from the MS, Thus, it will avoid transmission when the RS-MS link is bad, even though the BS-RS link might be good.

The IEEE 802.16m standard [1], [2] currently supports the hop-by-hop ARQ protocol for multihop cellular networks. In the hop-by-hop ARQ protocol, ARQ is performed separately on every multi-hop link. Thus, packets destined for the MS are first transmitted
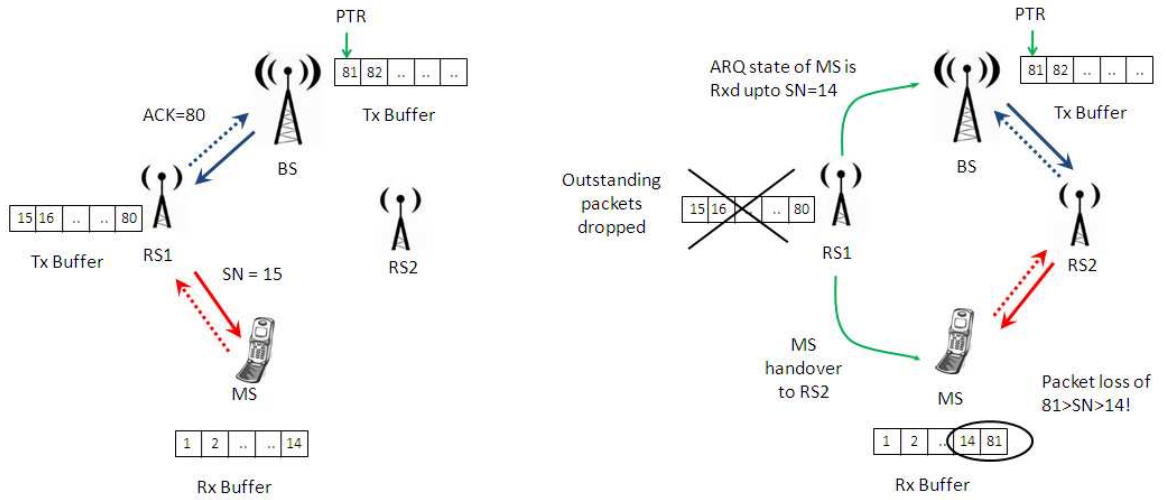
Figure 2.1: Illustration of packet loss during handover in hop-by-hop ARQ

by the BS to the RS. In case of packet loss or decoding error, RS sends a NACK to the BS asking for retransmission of the packet. In case of packet error on the RS-MS link, the RS performs the retransmissions to the MS. This protocol eliminates the low throughput performance and BS-RS link underutilization problems of the end-to-end ARQ scheme.

However, the BS is unaware of whether the packet has successfully reached the MS. It is only concerned with ensuring successful transmission of the packet on the BS-RS link. Due to this, hop-by-hop ARQ presents a major problem of packet loss in case of RS to BS or inter-RS handover. The problem has been illustrated in Fig. 2.1. When the BS receives ACK from the RS, it will clear the packets from its transmit buffer. The RS will maintain a queue of packets pending for transmission to the MS. Now if the MS hands over to the BS or another RS, the handoff target will not have a copy of these pending packets because the BS has already cleared them from its buffer. Transferring these packets from the RS to the BS and then to another RS will cause a huge signalling overhead and thus delay in handover. Thus, using the hop-by-hop ARQ protocol will result in gross packet loss in the event of RS to BS and inter-RS handover. In a relay-assisted cellular network, this packet loss will be high because of frequent handover of the MS between RSs.

As pointed out in a recent paper [20], very few studies have addressed handover issues in relay based cellular networks. In [21] the challenges in extending one-hop ARQ protocols to multi-hop are pointed out. A modified end-to-end ARQ protocol has been

proposed, but without supporting analytical or simulation results. In [22], hop-by-hop ARQ is modified such that the RS forwards NACKs from the MS to the BS. Theoretical and simulation analyzes of packet delay and ARQ transmission efficiency are presented. Later, [23] uses a Discrete-time Markov Chain (DTMC) model to analyze the packet loss due to buffer overflow at the BS and RS. However, issue of packet loss during inter-RS or RS-BS handover has not been considered in both [22] and [23]. To avoid packet loss during handover, [24] suggests a scheme in which the BS multicasts the data to all its subordinate RSs, so that when an MS hands over, the target RS has the data pending in queue at the serving RS. However, multicasting the data is a large signaling overhead and requires unnecessary buffer space at all the RSs.

In Chapter 5, we analyze the effect of handover on packet loss in hop-by-hop ARQ. Towards this, we propose a simple yet tractable channel model that captures the essentials of handover phenomenon. Using this model, we quantify the packet loss during handover in hop-by-hop ARQ. Finally, we propose modifications to hop-by-hop ARQ, and demonstrate how they help reduce packet loss during handover.

2.4   Handover Mechanism with Cellular Relays

In the next generation multi-hop cellular networks, non-transparent RSs support handover of MS to or from the BS or other RSs. But handover with an RS differs from inter-BS handover because of the absence of a backhaul directly connected to RSs. Consider the case of an RS-to-BS or an inter-RS handover. As discussed in the previous section, for hop-by-hop ARQ, the BS clears packets from its buffer after it receives an ACK from the RS, although the packets are still queued at the RS. These pending packets have to be communicated to the BS in case of RS-to-BS handover and to the target RS (via the BS) for an inter-RS handover. This causes a huge data transmission overhead, results in a large delay in handover. Only a few papers have addressed the design of the handover protocol for such a relay-assisted cellular system. [25] proposes a scheme in which the BS should multicast the packet to all the RSs. Thus, during handover, the target RS shall already have the packets present in the serving RS's queue. However, this scheme is not practically feasible because it involves too many unnecessary packet transmissions due the multicasting of data. The problem of designing handover protocols which prevent packet loss during handover with a low signalling overhead is open for future investigation.
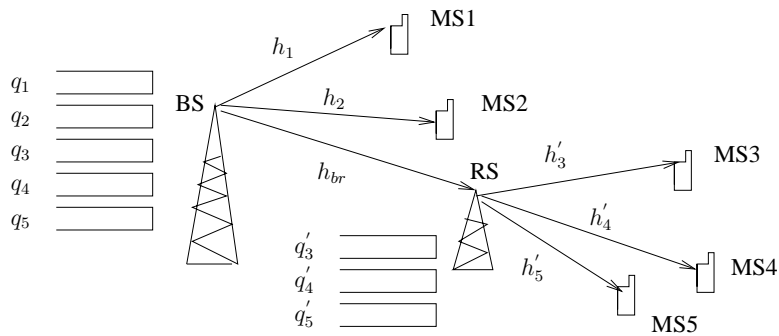
Figure 2.2: The delay-constrained scheduling problem in a relay-assisted cellular system

2.5 Scheduling with Delay Constraints

Developing an optimal scheduling policy for cooperative networks has been an interesting area of research for a few decades now. Various papers [26, 27, 28, 29, 30] have attempted to address this problem for ad-hoc networks. As described in Chapter 1, in next generation cellular networks with non-transparent RSs, there is no cooperative combining of packets from the direct and relay paths. Once an MS is handed over to an RS, all the further packets are sent via this RS, until another handover takes place. Thus, unlike ad-hoc networks, for relay-assisted cellular networks, the scheduling algorithm need not decide the route of every packet (i.e directly to MS or via RS), or the methods of combining multiple received copies of it. For cellular networks with RSs, we can develop simple heuristic scheduling policies to achieve the best network performance. [31, 32] present scheduling policies for such relay-assisted cellular scenarios.

In particular, scheduling with delay constraints is an interesting research problem. It has important application to scheduling of voice and video streaming traffic. [33] proposes an indexing scheduling algorithm for a simple one-hop multiuser scenario. It computes an index of each user, such that the index for the ith user is $\lambda_i = h_i(q_i - \delta_i)$ where h_i is the channel quality from the BS to the user, q_i is the queue length at the BS for the ith user, and δ_i is the desired queue length for that user, which corresponds for the delay constraint for that user.

In a relay assisted cellular system as shown in Fig. 2.2, two separate scheduling algorithms need to run at the BS and the RS, with periodic exchange of state information between them. For the MSs served via the RS, the scheduler at RS computed the index $\lambda_i = h_i'(q_i' - \delta_i')$ as described above. Similarly, for the MSs served directly by the BS

scheduler, the index $\lambda_i = h_i(q_i - \delta_i)$ as described above. However for MSs scheduled via RS, the BS scheduler needs to compute the index by taking into consideration the channel states and queue lengths for both the BS-RS and RS-MS links. Thus, in Fig. 2.2, the index λ_i for MS3, MS4 and MS5 is a function of h_{br}, h_i', q_i and q_i'. However, the challenge in designing this function is that the BS is not aware of the RS-MS channel states h_i', and queue lengths at RS, q_i'. Communication of the absolute values of these parameters by RS to the BS will cause a significant signaling overhead.

Thus, our objective is to design an index scheduling algorithm which computes the index for MSs served via RS with minimum status information exchanged between the RS and the BS. One idea is that each RS communicates the average queue length, i.e $q_{avg}' = E_i(q_i')$ and the ranks r_i based on the indices computed by the RS scheduler for serving its subordinate MSs. Using this information, the BS evaluates estimates q_i' and uses them to schedule the MSs served via the RS. Development and comparison of other such efficient protocols is open for future research.

2.6   Self Organizing Relays

Cellular operators are considering deployment of a new type of intelligent RSs in cellular networks - self-organizing RSs. Deployment of self-organizing RSs presents new challenges in analysis and design of next generation cellular networks. The main concept of self-organizing RSs is that they perform functions such as subcarrier allocation, power control and interference management autonomously, thus reducing the BS-RS communication overhead. Deployment of such RSs reduces the traffic load served by the BS and helps improve the system capacity. A futuristic property of self-organized RSs could also be the nomadic ability to move Self organizing RSs can be classified into two types - user-deployed and operator-deployed RSs. User-deployed RSs are placed by users in homes or offices to improve the network coverage in these spaces. Operator-deployed RSs are placed to improve signal quality in the coverage holes in the cell where high shadowing or penetration losses occur.

The key objective of research is to design self-organizing RSs which have autonomous functionalities to make them more independent of BS control. The following research problems can be formulated in terms of designing algorithms to make RSs more intelligent.

2.6.1 Subcarrier Assignment by Neighborhood Sensing

In case of fixed BSs, the subcarriers available in the cell are divided into disjoint sets which are allocated to the BS and each of the RSs, to use for their downlink transmissions. Instead of assigning disjoint sets, for every call arrival, the serving RSs can request the required subcarriers from the BS. The BS has the complete set of subcarriers from which it checks the availability of subcarriers requested and allocates them to the RS. However, this leads to signalling overhead between BS and RS. To avoid this, we can design a neighborhood sensing algorithm in which each RS measures the received interference power on each subcarrier and chooses the subcarriers with the minimum interference power for this transmissions. Further research can be done on analyzing the effect of the neighborhood sensing subcarrier allocation algorithm on the Erlang capacity of the system.

2.6.2 Autonomous Power Control for Interference Management

The transmit power of operator-deployed self-organized RSs is calibrated by the cellular operator, and the RSs are optimally placed such that coverage holes are served, while ensuring minimum interference to neighboring RSs. However, user-deployed self-organized RSs are placed at random locations in the cell. Thus, their coverage areas can overlap and cause interference to other RSs in the reference and neighboring cells. A possible research direction is to develop autonomous power control algorithms to minimize interference to neighboring RSs. Each RS can measure interference power from neighboring stations and scale it by the pathloss to the farthest MS served by it, to estimate the received SINR at that MS. It can then calibrate its power in order to satisfy a minimum threshold SINR at the farthest MS.

2.6.3 Relay Placement for Removal of Coverage Holes

Suppose the cellular operator wishes to deploy a new RS to improve coverage in areas which are not covered by the existing user-deployed and operator-deployed RSs. In this scenario, RS placement and power calibration is an improtant research issue. We can develop an algorithm which takes as input the existing RS positions and transmit powers and determines the optimal location of a new RS such it removes the maximum number

of coverage holes. Instead of applying brute force computation to the optimal location, we can apply learning algorithms to reduce the search space and arrive at a sub-optimal, but efficient solution.

Another problem is to determine locations of operator-deployed RSs, given a propagation loss profile at every point in the cell. We can develop an iterative algorithm where one RS is placed at the worst coverage hole in the cell. New RSs are added in an iterative fashion and are placed such that they remove the coverage holes not served by the existing RSs.

Chapter 3

Optimal Relay Placement for Coverage Extension

3.1   Introduction

As discussed in Chapter 2, optimal relay placement is an important research issue in next generation cellular networks. In this chapter is to present a novel formulation of the optimal cellular RS placement problem by defining the notion of the 'effective cell radius' of the cell in terms of the probability of correct decoding at a point. We determine the optimal RS position to achieve maximum effective cell radius, both for single cell and multi-cell scenarios. The multi-cell scenario takes into account inter-cell interference, which is a dominant factor in the next generation cellular Orthogonal Frequency Division Multiple Access (OFDMA) systems with 1:1 frequency reuse. The results presented in this chapter are useful to system planners for determining optimal values of parameters such as number, locations and transmit powers of cellular RSs.

The rest of the chapter is organized as follows. In Section 3.2, we describe the system model. In Section 3.3, we compute the optimal RS position to maximize the effective cell radius and estimate the number of RSs required in a relay-assisted cell. In Section 3.4, we extend this analysis to a multi-cell scenario with inter-cell interference and present an iterative algorithm to solve the problem. The results are presented in Section 3.5. In Section 3.6 we present an alternate formulation of the RS placement problem in which we determine the RS positions and transmit powers in a system where R_{eff} is already known. Finally, Section 3.7 concludes the chapter and provides directions for further investigation.

3.2   System Model
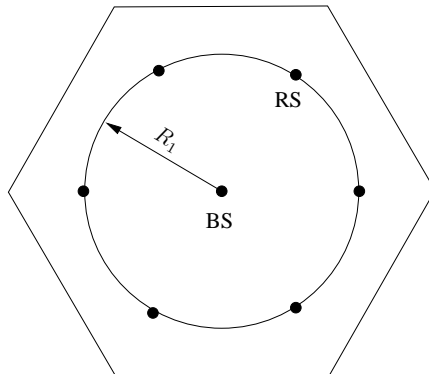
Figure 3.1: System topology in which each cell has a symmetrical ring of $N_R = 6$ RSs around the BS

We consider downlink data transmission in a relay-assisted cellular system. Cellular RSs can be classified into two broad types - transparent and non-transparent RSs. Transparent RSs do not transmit any pilot signals to the MS and hence the MS is unaware of their existence. A transparent RS functions like a repeater which merely forwards the signal from the BS to the MS. On the other hand, a non-transparent RS transmits pilot signals to the MS and performs most of the functions of a full-fledged BS such as inter-RS and RS-BS handover. The IEEE 802.16m standard [1] currently supports non-transparent RSs with no direct communication from BS to MS after the MS has been handed over to the RS.

We assume that N_R non-transparent RSs are placed symmetrically in a circular ring of radius R_1 around the BS in every cell as shown in Fig. 3.1. Although we focus our attention on the two-hop case with data transmission from the BS to MS via only one RS, our analysis can be extended to multi-hop relay architectures. The downlink transmit power of the BS is P_B dB and that of the RSs is P_R dB ($P_R < P_B$). The pathloss exponent in the system is denoted by η. The thermal noise level is N dBm. We consider log-normal shadowing on each link and denote it by ξ. ξ is a Gaussian random variable with mean 0 and standard deviation σ, σ_1 and σ_2 for the BS-MS, BS-RS and RS-MS links respectively. Since our aim is to evaluate the optimal RS positions from a long term coverage perspective, we ignore the effect of fast fading in the wireless channels.

Initially in Section 3.3, we consider a single cell scenario, and assume that there is no inter-cell interference from neighboring cells. The assumption of zero inter-cell interference
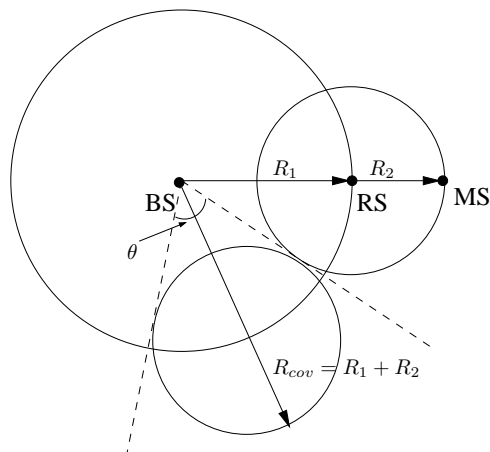
Figure 3.2: Illustration of the definition of effective cell radius R_{eff} for the relay-assisted cellular system. Also shown is the method to evaluate the angle θ subtended by each RS at the BS. $\theta = \sin^{-1}(R_2/R_1)$.

is relaxed in Section 3.4 where we analyze RS placement for a multi-cell scenario by taking into account the interference from the first tier of neighboring cells only.

3.3 Single Cell Scenario

Our objective is to determine the optimal radius of RS placement R_1 for which maximum cellular coverage is achieved. In this section, we solve this problem for a single cell scenario, without inter-cell interference from neighboring cells. This analysis is applicable to Global System for Mobile communications (GSM) cellular systems which employ frequency planning such that inter-cell interference is negligible. We determine the optimal R_1 and the approximate number of RSs required.

3.3.1 Effective Cell Radius

We first define cellular coverage by considering the example of a direct transmission from the BS to an MS at a radial distance d from it. As described in Section 3.2, we consider log-normal shadowing on each wireless link denoted by ξ (in dB). ξ is a Gaussian random variable with standard deviation σ on the BS-MS link. The received SNR at the MS is, $SNR_{BS-MS} = P_B - 10\eta \log d - N + \xi$. For correct decoding at the MS, the received SNR SNR_{BS-MS}, has to be greater than a decoding threshold T dB. Now we define p_c as the probability of correct decoding at a point. It is the probability that the received SNR is greater than threshold T. Thus, the probability of correct decoding of a signal at the MS

described in the example is,

$$
\begin{aligned}
p_c &= Pr(SNR_{BS-MS} > T) \\
&= Pr(P_B + \xi - 10\eta \log d - N > T) \\
&= Pr(\xi > T + N - P_B + 10\eta \log d) \\
&= Q\left(\frac{T + N - P_B + 10\eta \log d}{\sigma}\right).
\end{aligned}
\tag{3.1}
$$

where $Q(x) = \frac{1}{\sqrt{2\pi}} \int_x^\infty e^{-\frac{x^2}{2}} dx$. We define that a point is said to be covered if the probability of correct decoding p_c at that point, is greater than 0.5. Thus, the coverage area of the BS is a circular disc of radius R_{eff} such that $p_c \geq 0.5$ at all points inside it, and $p_c = 0.5$ at the circumference.

We define 'effective cell radius' R_{eff} as the maximum distance from the BS at which the MS experiences a probability of correct decoding $p_c = 0.5$, such that all locations of the MS at a radial distance greater then R_{eff} from the BS experience $p_c < 0.5$. In the example considered, when $p_c = 0.5 = Q(0)$, from (3.1), we have $T + N - P_B + 10\eta \log R_{\text{eff}} = 0$. Therefore, $R_{\text{eff}} = 10^{\frac{P_B - T - N}{10\eta}}$.

3.3.2 Relay Placement

We apply the definition of the effective cell radius R_{eff} to the relay-assisted cellular system described in Section 3.2. When an MS moves outside the coverage area of the BS, it is handed over to one of RSs in the cell, and starts receiving data from the BS via the RS. As per our definition, effective cell radius R_{eff} is the maximum distance from the BS for which transmission via an RS results in $p_c = 0.5$. R_{eff} will be maximum when the BS, RS and MS are collinear as shown in Fig. 3.2. $R_{\text{eff}} = R_1 + R_2$ where R_1 is the RS placement radius, and R_2 is the radius of the coverage disc of each RS in which MSs served by that RS experience probability of correct decoding greater than 0.5.

For transmission via RS, to be correctly decoded, RS has to correctly decode the signal received from the BS, and thereafter MS has to correctly decode the signal received from the RS. Thus, p_c at an MS located at $R_1 + R_2$ distance from BS as shown in Fig. 3.2 is a product of the corresponding probabilities, p_{c_1} on the BS-RS link and p_{c_2} on the

RS-MS link.

$$p_c = p_{c_1} . p_{c_2}$$
$$= Pr(SNR_{BS-RS} > T) \times Pr(SNR_{RS-MS} > T)$$
$$= Q\left(\frac{T + N - P_B + 10\eta \log R_1}{\sigma_1}\right) Q\left(\frac{T + N - P_R + 10\eta \log R_2}{\sigma_2}\right) \qquad (3.2)$$

At the distance $R_{\text{eff}} = R_1 + R_2$ from the BS, $p_c = p_{c_1} p_{c_2} = 0.5$. Given a RS placement radius R_1, R_2 is obtained as a function $f(R_1)$, by setting $p_c = 0.5$ in (3.2) as follows,

$$p_{c_1} = Q\left(\frac{T + N - P_B + 10\eta \log R_1}{\sigma_1}\right), \qquad (3.3)$$

$$R_2 = 10^{\left(\frac{P_R - N - T}{10\eta} + \frac{\sigma_2}{10\eta} . Q^{-1}\left(\frac{0.5}{p_{c_1}}\right)\right)}, \qquad (3.4)$$

$$= f(R_1). \qquad (3.5)$$

p_{c_1} is inversely proportional to the RS placement radius R_1. Therefore, if R_1 is large, p_{c_1} will take a small value and thus in order to maintain $p_{c_1} p_{c_2} = 0.5$, p_{c_2} will be large. Hence the distance from the RS to the cell edge, R_2 will be small. Thus there is a tradeoff between the values of R_1 and R_2. The effective cell radius $R_{\text{eff}} = R_1 + R_2$. Any MS at a radial distance greater than R_{eff} from the BS experiences a probability of success greater than or equal to 0.5. We determine the optimal RS placement radius R_1^* which maximizes the effective cell radius $R_1 + R_2$.

$$R_1^* = \arg \max_{R_1 \in (0, R_1^{max}]} R_1 + R_2 \quad \text{s.t. } p_{c_1} . p_{c_2} = 0.5,$$

$$R_2^* = f(R_1^*),$$

$$R_{\text{eff}}^* = R_1^* + R_2^*.$$

where, R_1^{max} is the distance of the RS from the BS where the probability of correct decoding, p_{c_1} is equal to 0.5. If RS is placed at a greater distance, it will not be possible to satisfy the condition $p_{c_1} . p_{c_2} = 0.5$. Thus,

$$R_1^{max} = 10^{\left(\frac{P_B - N - T}{10\eta} + \frac{\sigma_1}{10\eta} . Q^{-1}(0.5)\right)} = 10^{\left(\frac{P_B - N - T}{10\eta}\right)} \qquad (3.6)$$

3.3.3 Number of Relays

Now let us determine the approximate number of RSs required in the cell. We assume that the number of RSs is chosen such that the coverage discs of the RSs just touch each
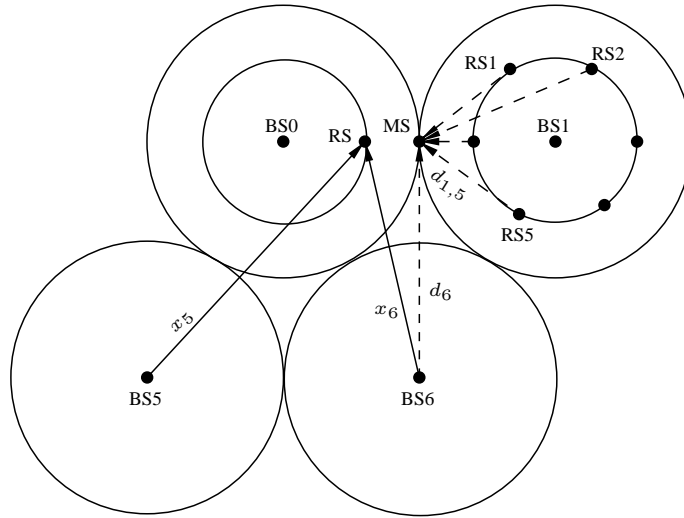
Figure 3.3: Illustration of the computation of ICI. Solid lines denote distances x_i from which the RS in the reference cell receives ICI from neighboring BSs. Dashed lines denote distances $d_{1,j}$ from which the MS receives ICI from the RSs in neighboring cell 1

other without overlapping, as shown in Fig. 3.2. Placing RSs such that their coverage discs are non-overlapping gives the minimum number of RSs required. There may be some coverage holes between adjacent RS coverage discs where the probability of correct decoding falls below 0.5. By increasing the number of RSs, the coverage holes can be reduced. The number of RSs required is inversely proportional to the coverage radius R_2 of each RS. Let the angle subtended by each RS's coverage disc at the BS be θ as shown in Fig 3.2. The approximate number of RSs required is,

$$N_R = \lceil \frac{2\pi}{\theta} \rceil$$
$$= \lceil \frac{\pi}{\sin^{-1}\left(\frac{R_2^*}{R_1^*}\right)} \rceil. \tag{3.7}$$

3.4 Multi-cell Scenario

Cellular OFDMA systems usually employ 1:1 frequency reuse. Inter-cell interference thus becomes significant and affects the optimal placement of RSs in the cell. In this section, we determine the optimal RS positions by taking into account the inter-cell interference. We assume inter-cell interference from the first-tier of neighboring cells only. In cellular OFDMA, a set of subcarriers, called a subchannel is allocated for each data transmission. Thus, in the OFDMA context, P_B and P_R shall denote power transmitted per subchannel by the BS and RS respectively. We assume that the BS-RS and RS-

MS links always transmit in orthogonal time or frequency slots. Thus, the MS receives inter-cell interference only from the RSs in the neighboring cells, and the RS receives interference only from the BSs of the neighboring cells. The inter-BS distance is equal to $2R_{\text{eff}}$. We assume a random subcarrier allocation algorithm employed in every cell for assigning subcarriers for data transmission on each of the links. Let p_{act} be the probability that a subcarrier is being used for data transmission in the cell. It depends upon the traffic load in each cell. We assume uniform traffic load across all the cells in the system. Hence p_{act} is constant across all cells in a multi-cell system with 1:1 frequency reuse.

3.4.1 Inter-cell Interference

Let us first evaluate the total interference power at an RS, I^r and at an MS at the cell edge I^m. For simplicity of the analysis of probability of correct decoding, we ignore shadowing on the interfering links and consider only the average interference power. We evaluate the total average interference power I^r received at the RS shown in Fig. 3.3. It is the sum of the average interference received from each neighboring BS I_i^r. To determine the average interference, we multiply the received power from an interfering BS by the probability of subcarrier activity p_{act}. Thus, the total interference at the RS is,

$$I^r = \sum_{i=1}^{6} I_i^r,$$
$$= \sum_{i=1}^{6} p_{act} P_B x_i^{-\eta}. \tag{3.8}$$

where $x_i = \sqrt{(2R_{\text{eff}})^2 + R_1^2 - 4.R_1.R_{\text{eff}}\cos(i\frac{\pi}{3})}$, the distance from the reference RS to the ith neighboring BS. Similarly, the interference power I^m received at an MS at the cell edge as shown in Fig. 3.3, is the sum of the sum of the interference received from each neighboring BS I_i^m, which in turn is the sum of the interference $I_{i,r}^m$ from each RS in the neighboring cells.

$$I^m = \sum_{i=1}^{6} I_i^m$$
$$= \sum_{i=1}^{6} \frac{p_{act}}{N_R} \sum_{r=1}^{N_R} P_R d_{i,r}^{-\eta} \tag{3.9}$$
$$\approx \sum_{i=1}^{6} \left(\sum_{r=1}^{N_R} P_R d_{1,r}^{-\eta} \right) \frac{d_i^{-\eta}}{d_1^{-\eta}} \tag{3.10}$$

where $d_{i,r}$ is the distance from the reference MS to the rth RS in the ith neighboring cell. For example, $d_{1,r} = \sqrt{R_{\text{eff}}^2 + R_1^2 - 2R_1.R_{\text{eff}}\cos(\frac{2\pi r}{N_R})}$. Since we assume a random subcarrier allocation algorithm, for the subchannel for the RS-MS transmission considered, each subcarrier has probability $1/N_R$ of being alloted to the rth RS in the ith neighboring cell. Hence we have the factor $1/N_R$ in (3.9). In (3.10), we determine the average interference power from the first neighboring cell, $i = 1$ and we scale it by the path loss $d_i^{-\eta}$ from the other neighboring BSs to the MS, to determine the approximate average interference from the other cells. Here, $d_i = \sqrt{4R_{\text{eff}}^2 + R_{\text{eff}}^2 - 4R_{\text{eff}}^2\cos(\frac{\pi i}{3})}$ is the distance from the reference MS to BS-i.

Algorithm 1 Iterative evaluation of R_1, N_R, R_{eff}

$R_{\text{eff}}^{(1)} \leftarrow R_{\text{eff}}^{(init)}$

$R_{\text{eff}}^{(0)} \leftarrow 0$

$N_R^{(1)} \leftarrow N_R^{init}$

$i \leftarrow 1$

while $R_{\text{eff}}^{(i)} - R_{\text{eff}}^{(i-1)} > \epsilon$ **do**

  for each $R_1 \in (0, R_{\text{eff}})$ **do**

    $\mathbf{R}_{\text{eff}} \leftarrow \{\emptyset\}$

    Compute I^r and I^m

    $p_{c_1} = Q\left(\frac{T+10\log(10^{\frac{N}{10}}+I^r)+10\eta\log R_1 - P_B}{\sigma_1}\right)$

    if $p_{c_1} < 0.5$ **then**

      break from for loop

    end if

    $p_{c_2} = Q\left(\frac{T+10\log(10^{\frac{N}{10}}+I^m)+10\eta\log R_2 - P_R}{\sigma_2}\right)$

    Solve $p_{c_1}.p_{c_2} = 0.5$ for R_2

    Append $(R_1 + R_2)$ to $\mathbf{R}_{\text{eff}}$

  end for

  $i \leftarrow i + 1$

  $R_{\text{eff}}^{(i)} = \max \mathbf{R}_{\text{eff}}$

  $R_1^{*(i)} = \arg\max \mathbf{R}_{\text{eff}}$

  $N_R^{(i)} = \lceil \frac{\pi}{\sin^{-1}(\frac{R_{\text{eff}}^{(i)} - R_1^{*(i)}}{R_1^{*(i)}})} \rceil$

end while

3.4.2   Relay Placement

In the single cell scenario, the SNR_{BS-RS} and SNR_{RS-MS} depend only the distances R_1 and R_2 and the respective transmit powers respectively as given in (3.2). However in the multi-cell scenario, since we consider inter-cell interference, the received signal to interference plus noise ratio (SINR) at the RS and MS is also a function of the inter-BS distance $2R_{\text{eff}}$, and the number of RSs N in every cell. Thus, we need to use an iterative Algorithm 1 to determine the RS placement radius R_1 that maximizes the cell coverage radius R_{eff}.

3.5   Results

In this section, we present the numerical results of the optimization problem formulated in Section 3.3 and Section 3.4. The system parameters are chosen according to Table I. In Fig. 3.4 we plot the effective cell radius $R_{\text{eff}} = R_1 + R_2$ versus the RS placement radius

SYSTEM PARAMETERS	
BS transmit power	$P_B = 36$ dBm
RS transmit power	$P_R = 28$ dBm
Path loss exponent	$\eta = 3.5$
Shadowing standard deviation BS-RS	$\sigma_1 = 3$ dB
Shadowing standard deviation RS-MS	$\sigma_2 = 6$ dB
Noise level	$N = -100$ dBm
Decoding Threshold SINR	$T = 10$ dB
Probability of subcarrier being active	$p_{act} = 0.2$

R_1. Given a value of R_1, R_2 is evaluated as shown in (3.11). We also plot the approximate number of RSs $N_R = \frac{\pi}{\sin^{-1}(R_2/R_1)}$. The maximum R_{eff} is attained approximately at $R_1 = 3550$ m. At this radial location of the RSs, $R_{\text{eff}} = 5475$ m. Thus the RSs are placed at $R_1^*/R_{\text{eff}} = 0.65$ fraction of the effective cell radius. Also, we evaluate from (3.7) that at the optimal value, 6 RSs are required to cover the cell area with minimum coverage gaps and without the coverage discs of RSs overlapping each other.

For the multi-cell scenario, we use the iterative Algorithm 1 to evaluate the optimal

RS placement radius R_1 and the corresponding R_{eff}. We set the initial values of $R_1^{(init)}$ and $R_{\text{eff}}^{(init)}$ to the R_1^* and R_{eff} determined in the single cell case. For the system parameters in Table I, and $\epsilon = 0.01$, the algorithm converges to the values $R_{\text{eff}} = 3900$ m and $R_1^* = 2338$ m. Fig. 3.6 shows the convergence of R_{eff} for different values of $P_R = 26, 27$ and 28 dBm. The R_{eff} reduces as compared to the single cell case due to inter-cell interference from the neighboring cells.

In Fig. 3.5 we plot the ratio R_1^*/R_{eff}^* versus the RS transmit power P_R, for the single cell and multi-cell scenarios. The BS transmit power is constant at $P_B = 36$ dBm. As the P_R increases the RS can serve MS further away from it, and hence the ratio decreases. We also observe that the ratio is greater for the single cell case. In the multi-cell scenario, the optimal RS radius moves away from the cell edge in order to reduce the interference to neighboring cells.
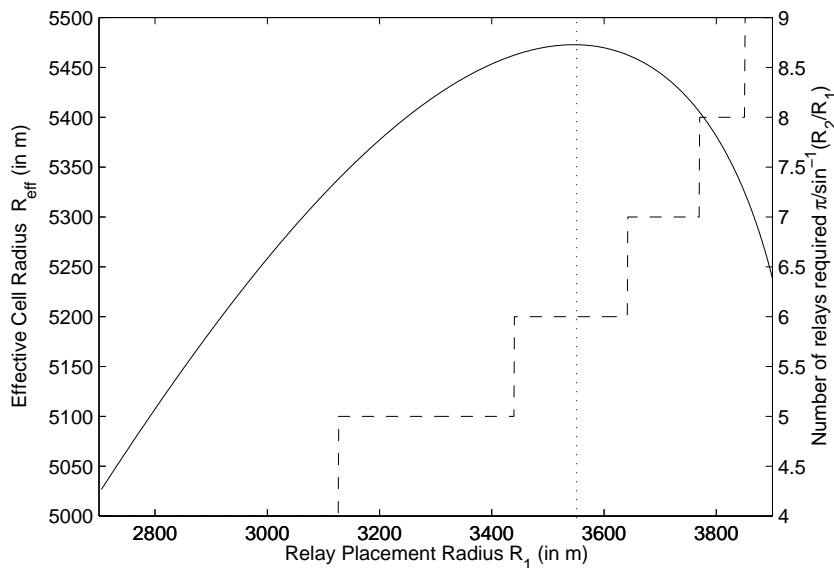
Figure 3.4: Plots of effective cell radius R_{eff} and number of RSs N_R versus the RS placement radius R_1.

3.6   An Alternate Problem Formulation

So far, we have considered the problem where, given the transmit powers of the BS and RS, we have determined the RS placement radius R_1 which maximizes the effective coverage radius R_{eff}. However, in practice the cellular operator would like to place RSs in an already deployed system, where is the inter-BS distance and hence, the cell radius R_{eff}
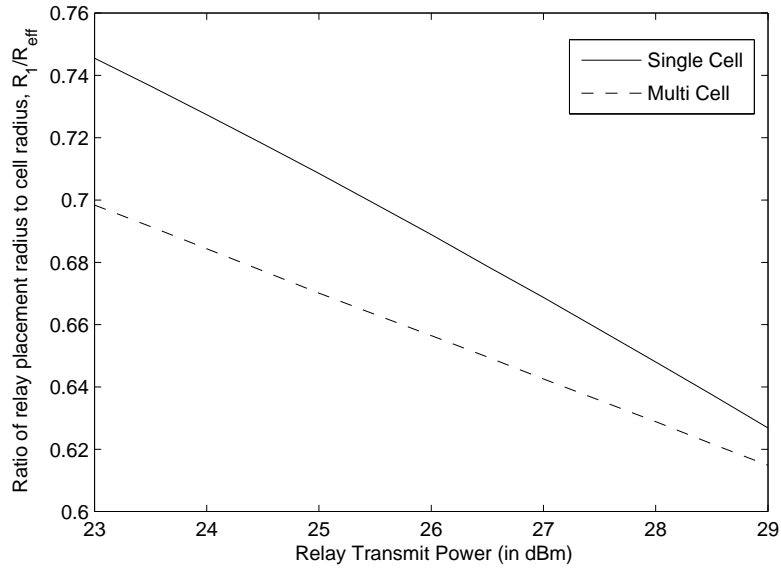
Figure 3.5: Plots of the ratio R_1/R_{eff} versus RS transmit power for the single cell and multi-cell scenarios.
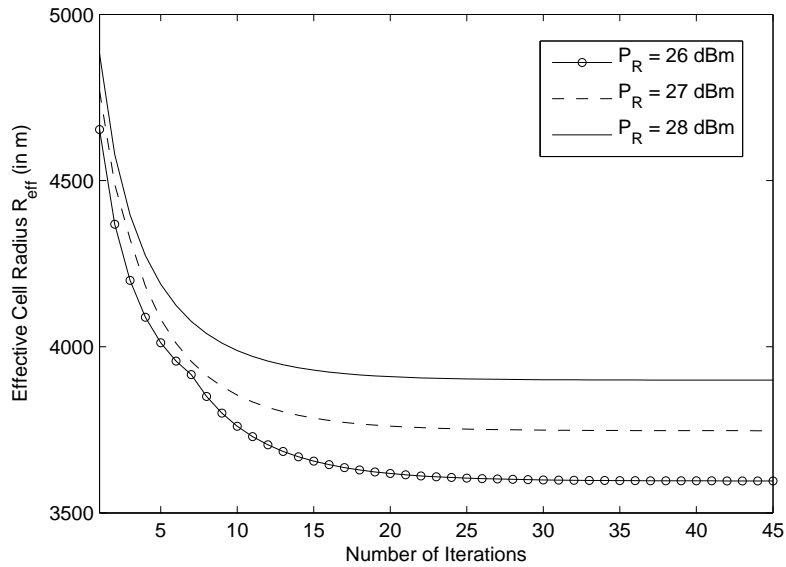
Figure 3.6: Plots demonstrating the convergence of R_{eff} in the iterative algorithm proposed to determine the optimal R_1 in the multi-cell scenario.

is already known. In such a case, we can reformulate the problem as that of determining the optimal RS position R_1 to cover the given cell area of radius R_{eff} with the minimum RS transmit power P_R. This idea can be applied both to the single cell and the multi-cell scenarios.

For the single cell scenario, given an RS placement radius R_1, P_R is obtained as a

function $g(R_1)$, by setting $p_c = 0.5$ in (3.2) as follows,

$$p_{c_1} = Q\left(\frac{T + N - P_B + 10\eta \log R_1}{\sigma_1}\right),$$

$$p_{c_2} = \frac{0.5}{p_{c_1}} = Q\left(\frac{T + N - P_R + 10\eta \log(R_{\text{eff}} - R_1)}{\sigma_2}\right),$$

$$P_R = \sigma_2.Q^{-1}\left(\frac{0.5}{p_{c_1}}\right) - N - T - 10\eta \log(R_{\text{eff}} - R_1),$$

$$= g(R_1). \tag{3.11}$$

Then, we solve the following optimization problem and determine the optimal R_1^* for which the P_R required in minimum.

$$R_1^* = \arg \min_{R_1 \in (0, R_1^{max}]} P_R \quad \text{s.t. } p_{c_1}.p_{c_2} = 0.5.$$

For this alternate problem formulation we plot the RS transmit power P_R versus the RS placement radius R_1 in Fig. 3.7. The effective cell radius $R_{\text{eff}} = 5000$ m. The minimum P_R is 23.5 dB and is attained at $R_1 = 3680$ m.
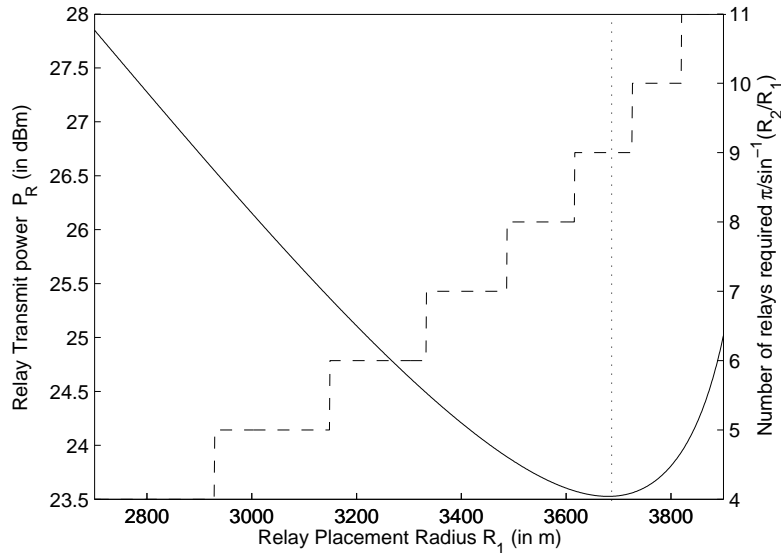
Figure 3.7: Plots of RS transmit power P_R and number of RSs N_R, versus R_1

3.7 Conclusions

In this chapter we have analyzed of RS placement in cellular networks for maximum coverage improvement. The optimization problem is solved both for the single cell and

multi-cell scenarios. We present a novel approach to determine the optimal RS positions by defining the effective cell radius in terms of the probability of correct decoding at a point. For the multi-cell scenario we take into account inter-cell interference and propose an iterative algorithm to determine the optimal RS positions. The results presented in this paper can be used by cellular operators, we determine the RS positions for maximum extension of cell radius.

We have considered a downlink cellular transmission and determined the optimal RS position for it. Solving the analogous uplink problem may yield a different optimal RS position. But, the uplink and downlink transmit powers of each RS can be adjusted in order to cause these two optima to coincide. This could be a direction for future investigations. Another possible research direction is to extend the two-hop analysis in this work to the multi-hop relay case.

Chapter 4

Capacity Improvement of Cellular OFDMA

4.1 Introduction

As discussed in Chapter 2, introduction of RSs can help improve the Erlang capacity of cellular OFDMA. In this chapter, we present a novel approach to evaluate the downlink Erlang capacity of cellular OFDMA. Incoming users are divided into various classes based on their subcarrier requirement. To determine the arrival rate for each class, we compute the probability distribution of the number of subcarriers required by an incoming user. We then model the system as a multi-dimensional Markov chain and compute blocking probability and Erlang capacity of the system. We extend the analysis to Erlang capacity evaluation for a relay-assisted cellular system and demonstrate how introduction of cellular relays improves the capacity of the system. We then study the effect of BS-RS bandwidth distribution, and the location of relays on the blocking probability and Erlang capacity. These results can be used by cellular operators for the design of relay-assisted cellular networks.

The rest of the chapter is organized as follows. In Section 4.2, we formulate and solve the Erlang capacity determination problem for a cellular OFDMA system without relays. This section is collaborative work with Harshad Maral and has also been included in the thesis [34]. In Section 4.3, we extend this analysis to a relay-assisted cellular OFDMA system. We present simulation setup and experimental results in Section 4.4. Finally, we conclude the chapter in Section 4.5 and provide directions for further investigations.

4.2   Erlang Capacity of cellular OFDMA

In this chapter, we evaluate the Erlang capacity of cellular OFDMA using the unique approach of dividing incoming calls into classes. The system model is presented in Section 4.2.1. We then formulate the problem and present the solution in Sections 2 and 4.2.3 respectively.

4.2.1   System Model

We consider a cellular OFDMA system with circular cells of radius R as shown in Fig. 4.1. Cell 0 is the reference cell and cells 1 to 6 are its neighbors. Users are assumed to be uniformly distributed in the circular area of each cell. Call arrivals in each cell are Poisson distributed with rate λ, and the call holding times are exponentially distributed with mean $\frac{1}{\mu}$. We assume that all incoming calls have a rate requirement (normalized by the subcarrier bandwidth) of R_{req} bits/sec/Hz. Though we do not consider multi-service traffic where each class of users has a different rate requirement, our analysis can be extended to such a scenario.

The BS in each cell has N subcarriers available for allocation to the mobile stations (MSs) in the cell for downlink data transmission. The BS transmits at constant power P_{tx} on each subcarrier. The downlink signal to noise plus interference ratio (SINR) on each subcarrier depends upon the location of the MS in the reference cell, channel fading and interference from neighboring cells. We consider log-normal shadowing on each subcarrier, with mean 0 and standard deviation σ. Fast fading is ignored since our aim is to evaluate the Erlang capacity from a long term capacity planning perspective. For
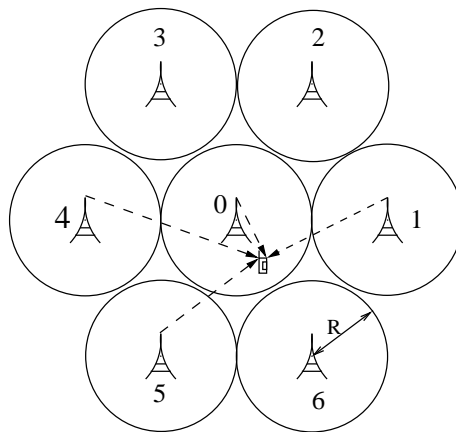
Figure 4.1: Illustration of the inter-cell interference on one subcarrier allocated to the MS in cell 0, coming from the BSs where that subcarrier is in use

modeling inter-cell interference, we consider a 1:1 frequency reuse pattern, and assume that the interference occurs from only the first-tier of neighboring cells, i.e cells 1 to 6 in Fig. 4.1.

4.2.2   Problem Formulation

Our aim is to determine the Erlang capacity of cellular OFDMA. Erlang capacity is defined as the traffic load in Erlangs supported by the cell while ensuring that blocking probability is below a certain value. By determining the blocking probability as a function of the offered load in Erlangs, we can evaluate the Erlang capacity of the cell.

In a GSM or any standard circuit switched system which can support N calls simultaneously, every incoming call occupies only one circuit and releases it on departure. The system is said to be in state i when it has i active calls. This system state can be modeled as a one-dimensional continuous time Markov chain. The blocking probability P_B is the steady state probability of the system being in state N and is given by the standard Erlang-B formula $P_B = \frac{\frac{\rho^N}{N!}}{\sum_{i=0}^{N} \frac{\rho^i}{i!}}$ where $\rho = \frac{\lambda}{\mu}$ is the offered Erlang load. However, this analysis cannot be applied to cellular OFDMA where the number of subcarriers required, n_{req} is a function of the downlink SINR on each subcarrier. Let $SINR_i$ be the downlink SINR on i^{th} subcarrier in the reference cell. Then,

$$SINR_i = \frac{P_{\mathrm{tx}} D^{-\eta} 10^{\frac{\xi}{10}}}{I_i + N_0}, \quad 1 \leq i \leq N, \tag{4.1}$$

where P_{tx} is the power transmitted by the BS on i^{th} subcarrier, D is the radial distance of the MS from the BS and η is the path loss exponent. ξ models the shadowing on the BS-MS link and is a Gaussian random variable with mean 0 and standard deviation σ. N_0 is the thermal noise density and I_i is the total interference received on i^{th} subcarrier. Let $I_{i,j}$ be the interference from j^{th} neighboring cell where $1 \leq j \leq 6$. Then,

$$I_i = \sum_{j=1}^{6} I_{i,j} \mathbf{1}_A(i,j) \tag{4.2}$$

$$= \sum_{j=1}^{6} P_{\mathrm{tx}} D_j^{-\eta} 10^{\frac{\xi_j}{10}} \mathbf{1}_A(i,j) \tag{4.3}$$

where $\mathbf{1}_A(i,j)$ is an indicator random variable which takes the value 1 if i^{th} subcarrier has been allocated to an MS in j^{th} neighboring cell, and 0 otherwise. D_j is the distance

between the BS of jth neighboring cell and the MS in the reference cell and ξ_j is the shadowing factor on this link.

When there is a call arrival in the reference cell, the BS allocates a set of subcarriers to the MS in order to just satisfy the user's rate requirement R_{req}. Thus the number of subcarriers required, n_{req} is random and is such that,

$$\sum_{i=1}^{n_{\text{req}}} \log_2(1 + SINR_i) \geq R_{\text{req}}. \tag{4.4}$$

An incoming call is blocked if the number of subcarriers available at BS is less than n_{req}. Further, we assume that once a set of subcarriers is allocated to the MS, it uses them for the entire call duration, and the subcarriers are released when the call departs. Our objective is to determine the call blocking probability by taking into account the randomness in n_{req}.

4.2.3   Solution Strategy

In this section, we describe our approach to determine the blocking probability for the cellular OFDMA system. The key idea is to divide incoming calls into classes according to their subcarrier requirement n_{req}. The arrival rate for a class of calls requiring n subcarriers is the product of the arrival rate λ for the cell and the probability that the call requires n subcarriers. This probability is obtained from the probability distribution function of n_{req}, the number of subcarriers required by an incoming call.

Distribution of number of subcarriers required

We assume the random subcarrier allocation scheme given in Algorithm 2 where the BS arbitrarily chooses n_{req} subcarriers from the available set and allots them to an incoming user[1]. The BS chooses one subcarrier randomly from the available set and checks whether the user's rate requirement is satisfied by it, that is whether $\log_2(1 + SINR)$ for that subcarrier is greater than or equal to R_{req}. If not, it continues to add randomly chosen subcarriers until the total rate over the set of subcarriers becomes greater than or equal to R_{req}. This set of n_{req} subcarriers is then allocated to the user. If the available set of subcarriers cannot meet the rate requirement, the call is blocked. We assume that the

---

[1]We assume that subcarrier allocation is not in chunks, and the BS can allocate any integer number of subcarriers to the users. However the analysis can be extended to chunk allocation.

Algorithm 2 Subcarrier allocation scheme

---

for each call arrival **do**

    $R_{\text{temp}} \leftarrow 0$

    $n_{\text{allot}} \leftarrow 0$, number of subcarriers to be allocated

    $\mathbf{S}_{\text{avail}}$: set of available subcarriers in the cell

    $\mathbf{S}_{\text{allot}} \leftarrow \{\}$, set of subcarriers to be allocated

    $\mathbf{S}_{\text{temp}} \leftarrow \mathbf{S}_{\text{avail}}$

    while $\mathbf{S}_{\text{temp}} \neq \{\}$ do

        Choose randomly subcarrier $s \in \mathbf{S}_{\text{temp}}$

        $\mathbf{S}_{\text{temp}} \leftarrow \mathbf{S}_{\text{temp}} - s$

        $n_{\text{allot}} \leftarrow n_{\text{allot}} + 1$

        $\mathbf{S}_{\text{allot}} \leftarrow \mathbf{S}_{\text{allot}} + s$

        $R_{\text{temp}} \leftarrow R_{\text{temp}} + \log_2\left(1 + SINR_s\right)$

        if $R_{\text{temp}} \geq R_{\text{req}}$ then

            Allocate $\mathbf{S}_{\text{allot}}$ to arriving call

            $\mathbf{S}_{\text{avail}} \leftarrow \mathbf{S}_{\text{avail}} - \mathbf{S}_{\text{allot}}$

            $n_{\text{req}} \leftarrow n_{\text{allot}}$

            break

        else if $\mathbf{S}_{\text{temp}} = \{\}$ then

            Block the arriving call

        end if

    end while

end for

MS uses the set of allocated subcarriers for the entire duration of the call. When the call ends, the subcarriers are released into the available set.

We determine $f_n[n_\text{req}]$, the discrete probability distribution function of the number of subcarriers required by an incoming call for $1 \leq n_\text{req} \leq N$. For an n_req, $f_n[n_\text{req}]$ is the probability that an incoming call in the system requires n_req subcarriers to satisfy its rate requirement.

Computation of blocking probability

In this section we use the probability distribution function determined previously, to evaluate the Erlang capacity of the cell. Let $f_n[n_\text{req}]$ be non-zero for K values of n_req, $\{n_1, n_2, ..n_K\}$. Hence we divide incoming calls into K classes such that a call belongs to class-i if it requires $n_\text{req} = n_i$ subcarriers to satisfy its rate requirement. The rate of Poisson call arrivals in the cell is λ. Thus, by the probability distribution $f_n[n_\text{req}]$, we can infer that the arrival rate of calls of class-i is $\lambda_i = \lambda f_n[n_i]$. The holding time for all classes of calls is exponentially distributed with mean $\frac{1}{\mu}$. Thus, the offered load for class-i is $\rho_i = \rho f_n[n_i]$.

We model the system by a K-dimensional Markov chain where the system state is defined as $\mathbf{X} = (X_1, X_2, ..X_K)$ where X_i is the number of active calls belonging to class i (i.e. using n_i subcarriers each). N is the total number of subcarriers available in the cell. As an illustrative example, consider the Markov chain shown in Fig. 4.2 with $N = 4$ subcarriers and $K = 2$ classes of calls. Calls require $n_1 = 1$ subcarrier with probability $f_n[1] = 0.6$ and $n_2 = 2$ subcarriers with probability $f_n[2] = 0.4$. Thus, the arrival rate of class-1 calls is 0.6λ and that of class-2 is 0.4λ.

The steady state probability of state $\mathbf{x} = (x_1, x_2, ...x_K)$ is defined as $\pi(\mathbf{x}) = P(\mathbf{X} = \mathbf{x})$. When $\mathbf{X} = \mathbf{x}$, the number of subcarriers in use by the active calls in the system is,

$$N_\text{used} = \sum_{i=1}^{K} n_i x_i, \tag{4.5}$$

$$= \mathbf{n}.\mathbf{x}, \tag{4.6}$$

where $\mathbf{n} = (n_1, n_2, ...n_K)$. Thus, the set of possible states of the system is,

$$\mathcal{S} := \{\mathbf{X} = \mathbf{x} : \mathbf{n}.\mathbf{x} \leq N\} \tag{4.7}$$
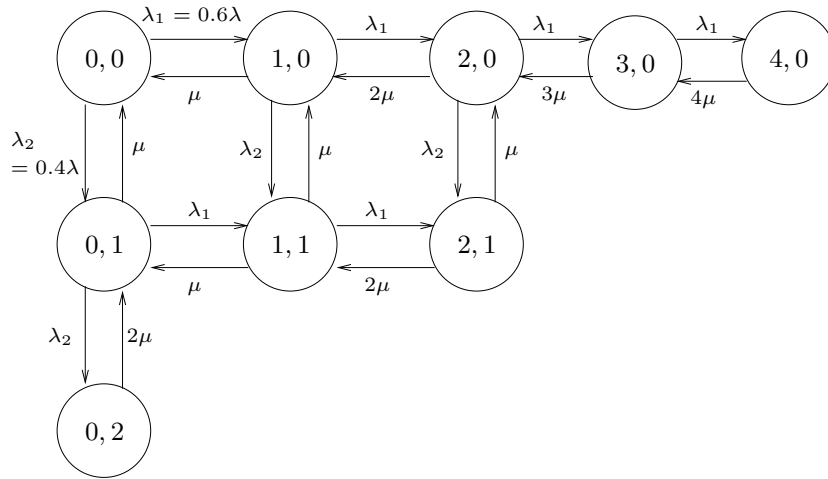
Figure 4.2: Markov chain model for a system with $K = 2$ and $N = 4$. Incoming calls are divided into 2 classes since n_{req} takes 2 possible values.

Let $\mathcal{S}_i$ be the subset of states in which an incoming call of class i will be blocked. Thus,

$$\mathcal{S}_i := \{\mathbf{x} \in \mathcal{S} : \mathbf{n}.\mathbf{x} > N - n_i\} \tag{4.8}$$

For example, in Fig. 4.2 the subset of states in which an incoming call of class-1 will be blocked is $(4, 0)$, $(2, 1)$ and $(0, 2)$. The sum of the steady state probabilities of this subset is equal to the blocking probability for class-1. For the cellular OFDMA system with K classes, the blocking probability for class-i arrivals can be expressed as,

$$P_{B_i} = \sum_{\mathbf{x} \in \mathcal{S}_i} \pi(\mathbf{x}). \tag{4.9}$$

Following [35], this can be shown to be equal to,

$$P_{B_i} = \frac{\sum_{\mathbf{x} \in \mathcal{S}_i} \prod_{j=1}^{K} \frac{\rho_j^{x_j}}{x_j!}}{\sum_{\mathbf{x} \in \mathcal{S}} \prod_{j=1}^{K} \frac{\rho_j^{x_j}}{x_j!}}. \tag{4.10}$$

Due to large size of the state spaces, the evaluation of the blocking probability by brute force computation of all the steady state probabilities in (4.10) is practically infeasible. We solve this problem by drawing an analogy between the cellular OFDMA system and the stochastic knapsack in [35]. The stochastic knapsack is a generalization of the classical knapsack problem. It consists of a fixed number of resource units N to which objects of K classes with heterogeneous resource requirements arrive. Objects of class i require n_i resource units, their arrival rate is λ_i and mean holding time is $\frac{1}{\mu_i}$. We

model the cellular OFDMA system as a stochastic knapsack by choosing $\lambda_i = \lambda f_n[n_i]$ and $\mu_i = \mu$. A recursive algorithm to efficiently evaluate the blocking probability of class i objects is presented in [35]. We use this algorithm to determine the blocking probability P_{B_i} of class i calls. Intuitively we can see that P_{B_i} would be higher for a class of calls requiring larger number of subcarriers n_i, because the subset of states $\mathcal{S}_i$ for which an incoming call is blocked is larger. Since $f_n[n_i]$ is the probability that an incoming call belongs to class i, the average blocking probability for the system is,

$$P_B = \sum_{i=1}^{N} P_{B_i} f_n[n_i], \quad 1 \le i \le K. \tag{4.11}$$

Thus, we have obtained the blocking probability for a given value of offered load ρ. It is used to evaluate the Erlang capacity of the cellular OFDMA system.

4.3   Erlang Capacity of cellular OFDMA with Relays

Now we extend the analysis of Erlang capacity of cellular OFDMA to a relay-assisted cellular system. The main difference between these two cases is that with relays, one needs to check subcarriers availability both on the BS-RS and the RS-MS links.

4.3.1   System Model

Consider a downlink transmission in the relay-assisted cellular system as shown in Fig. 4.3. M relays are placed in a symmetrical ring around the BS at a distance 3/4rds of the cell radius R. The transmit powers for BS and RS are P_B dBm and P_R dBm respectively. We assume that if a user is at a distance d_b from the BS and d_r from the nearest RS such that $(P_B - 10\eta \log d_b) > (P_R - 10\eta \log d_r) + \Delta P$, then the user is served by the BS directly. Otherwise, it is served by the BS via the RS. We define ΔP as the MS association power. A call is served directly by the BS if the received signal strength from the BS is ΔP dB higher than that received from the nearest RS.

Let the total subcarriers available in the cell be N_{cell}. We assume a subcarrier distribution policy in which the subcarriers are divided into $M+1$ disjoint sets for downlink transmission of the BS and RSs in each cell. The subcarrier frequencies in each set are uniformly chosen from the N_{cell} available subcarriers in every cell. N_{RS} subcarriers are reserved for each RS, and are alloted for RS-MS packet transmissions. Similarly, the BS

has $N_{BS} = N_{cell} - M.N_{RS}$ subcarriers available for allotment to BS-RS and BS-MS packet transmissions.

All other system parameters such as call arrival and departure rates, rate requirement and inter-cell interference model are same as described in Section 4.2.1.
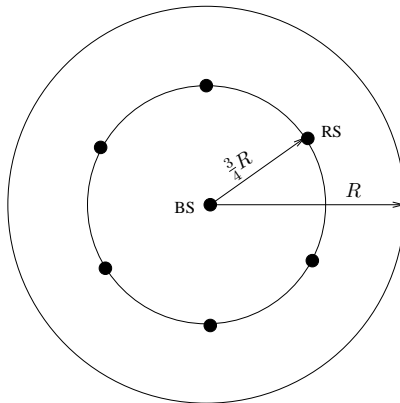
Figure 4.3: System Topology

4.3.2 Distribution of Subcarriers

To determine the Erlang capacity of the cellular OFDMA system with relays, we extend the idea of dividing calls into classes depending upon their subcarrier requirement similar to the analysis in Section 4.2. In the previous case, subcarriers were allotted for the BS-MS transmission of each call. However, for a relay-assisted cellular system, we have BS-MS, BS-RS and RS-MS packet transmissions.

In order to take into account all these links, we divide incoming calls into two type, Type I and Type II. Calls of Type I are served by the BS directly, and Type II calls are served via one of the RSs in the cell. For a call of Type II to be admitted to the system, sufficient subcarriers to satisfy the rate requirement R_{req} should be available both on the BS-RS and RS-MS links. We consider the BS-RS and RS-MS data transmissions as two separate calls and denote them as calls of Type IIA and IIB respectively. Thus, a call arrival of Type II implies the arrival of one call each of Type IIA and Type IIB.

In Section 4.2.3 we determine the probability distribution of the number of subcarriers required by a call, to satisfy the user's rate requirement R_{req}. For a call via the RS to be admitted to the system, sufficient subcarriers to satisfy the rate requirement R_{req} should be available both on the BS-RS and RS-MS links. N_{BS} subcarriers are shared by

Type I and Type IIA calls. At the serving RS, N_{RS} subcarriers are used for allocation to incoming Type IIB calls. By using analysis similar to Section 4.2.3, we determine the probability distributions of n_{req}, $f_1[n]$, $f_{2a}[n]$, and $f_{2b}[n]$ for the BS-MS, BS-RS and RS-MS links respectively.

4.3.3   Computation of Blocking Probability

From the condition $(P_B - 10\eta \log d_b) > (P_R - 10\eta \log d_r) + \Delta P$, let a fraction x of the total calls arrivals be served directly by the BS. Thus, if the call arrival rate in the cell is λ, then the rate of arrivals of calls for Type I is $\lambda_1 = x\lambda$ and for Type II is $\lambda_2 = (1-x)\lambda$. From the assumption of uniform distribution of users, the Type II are equally distributed across the M RSs in the cell. Thus, the arrival rate of Type II calls in the coverage area of each RS is, $\frac{\lambda_2}{M}$.

Let the blocking probabilities for calls of Type I and II be p_B^I and p_B^{II} respectively. The overall call blocking probability is, $p_B = x.p_B^I + (1-x).p_B^{II}$. A call of Type II is blocked if the subcarrier requirement is not satisfied on either of the BS-RS, and RS-MS links. Hence, the blocking probability for Type II is,

$$p_B^{II} = 1 - (1 - p_B^{IIA})(1 - p_B^{IIB}) \tag{4.12}$$

$$= p_B^{IIA} + p_B^{IIB} - p_B^{IIA}.p_B^{IIB} \tag{4.13}$$

Now let us determine the blocking probabilities, p_B^I, p_B^{IIA} and p_B^{IIB} in order to determine the overall call blocking probability for the cell. First consider Type IIB, corresponding to allotment of N_{RS} subcarriers to incoming calls. We have the distribution $f_{2b}[n_{\text{req}}]$ of the number of subcarriers required, n_{req}. Let $f_{2b}[n_{\text{req}}]$ be non-zero for K_{2b} values of n_{req}, $\{n_1, n_2, .. n_{K_{2b}}\}$. Hence we divide incoming calls of Type IIb into K_{2b} classes such that a call belongs to class i if it requires $n_{\text{req}} = n_i$ subcarriers to satisfy its rate requirement. The arrival rate of calls of class i is $\frac{\lambda_2}{M} f_{2b}[n_i]$. The holding time for all classes of calls is exponentially distributed with mean $\frac{1}{\mu}$. Thus, the offered load for class i will be ρ_i. We model the system by a K_{2b}-dimensional Markov chain and perform the same analysis using the idea of a stochastic knapsack as given in Section 4.2.3 to determine the blocking probabilities p_{B_i}. Thus, $p_B^{IIB} = \sum_{i=1}^{K_{2b}} p_{B_i}^{IIb}.f_{2b}[n_i]$.

Type I and Type IIA calls share the N_{BS} subcarriers available for allocation at the BS. Let the distributions $f_1[n_{\text{req}}]$ and $f_{2a}[n_{\text{req}}]$ be non-zero for K_1 and K_{2a} values of

n_req respectively. Denote these values by $\{n_1, n_2, .. n_{K_1}\}$ and $\{n_{K_1+1}, n_{K_1+2}, .. n_{K_1+K_{2a}}\}$ respectively. We divide calls into $K_1 + K_{2a}$ classes such that a call of class i requires n_i subcarriers where $i \in [1, K_1 + K_{2a}]$. Following the same approach as in Section 4.2.3, we determine the blocking probabilities p_{B_i} for each class. Thus, the blocking probabilities for Type I and Type IIa are,

$$p_B^I = \sum_{i=1}^{K_1} p_{B_i}.f_1[n_i], \qquad (4.14)$$

$$p_B^{IIA} = \sum_{i=K_1+1}^{K_1+K_{2a}} p_{B_i}.f_{2a}[n_i]. \qquad (4.15)$$

4.4 Experimental Evaluation

In this section, we describe the system-level simulations performed to determine $f_n[n_\text{req}]$. This distribution is used to compute the arrival rate for each class of calls as defined in Section 4.2.3. Then using the recursive algorithm in [35], we numerically compute the blocking probability P_B. The simulation results of $f_n[n_\text{req}]$ and the numerically computed blocking probability and Erlang capacity are presented. Specifically, we demonstrate the effect of rate requirement and power transmitted by BSs on the Erlang capacity of the system.

4.4.1 Simulation Setup

We consider downlink transmissions in a cellular OFDMA network of circular cells of radius R each. We assume inter-cell interference from BSs of the first-tier of neighboring cells only. The values of system parameters chosen for simulations are given in Table I. We generate the arrival and departure events of a large number of calls in the reference cell and each of the 6 neighboring cells. The call arrivals are Poisson with rate λ and holding times are exponentially distributed with mean $\frac{1}{\mu}$ in all cells. To achieve uniform spatial distribution of users in a circular cell, we generate the radial position (D, θ) of the MS for each call arrival by drawing θ from a uniform distribution in $[-\pi, \pi]$ and D from $f_D(d)$ where

$$f_D(d) = \frac{2d}{R^2}, \quad 0 \le d \le R. \qquad (4.16)$$

Table 4.1:

SYSTEM PARAMETERS	
Cell Radius	$R = 1000$ m
Subcarriers available in each cell	$N = 512$
Power transmitted by BS per subcarrier	$P_{\text{tx}} = 10$ dBm
Path loss exponent	$\eta = 3.5$
Shadowing standard deviation	$\sigma = 8$ dB
Thermal noise density	$N_0 = -100$ dBm

For every call arrival, we use the subcarrier allocation scheme in Algorithm 2 to allocate n_{req} subcarriers to the incoming call. For this, we need to determine the $SINR$ on each of the available subcarriers as given in (4.1). To evaluate the interference power I_i on a subcarrier i, we check whether it has been allocated to an MS in any of the neighboring cells. If subcarrier i has been allocated in cell j, the interference power received at the MS from j^{th} BS is added to the total inter-cell interference on that subcarrier. For each call which is admitted to the system we note the interference increase for the neighboring cells on the alloted set of subcarriers. For every call departure, we release the set of subcarriers occupied by the call into the set of available subcarriers in that cell. Also, the inter-cell interference caused to the neighboring cells on the released set of subcarriers is set to zero.

As a result of this simulation, we obtain a large number of values of n_{req} for the given system parameters. We use these values to determine $f_n[n_{\text{req}}]$. For a given n_{req}, $f_n[n_{\text{req}}]$ is the fraction of call arrivals for which the number of subcarriers required is n_{req}. We obtain the call arrival rates of each class of users from this distribution as explained in Section 4.2.3. The arrival rate for class i is $\lambda f_n[n_i]$.

4.4.2   Erlang Capacity without relays

The probability distribution $f_n[n_{\text{req}}]$ is plotted in Fig. 4.4 for different values of rate requirement R_{req}. We observe that for higher values of R_{req}, the average number of subcarriers required by users is higher. For each curve, the calls requiring larger number of subcarriers correspond to the users either located at the cell edge, or experiencing a deep fade. Using $f_n[n_{\text{req}}]$ we determine the blocking probability as a function of the offered
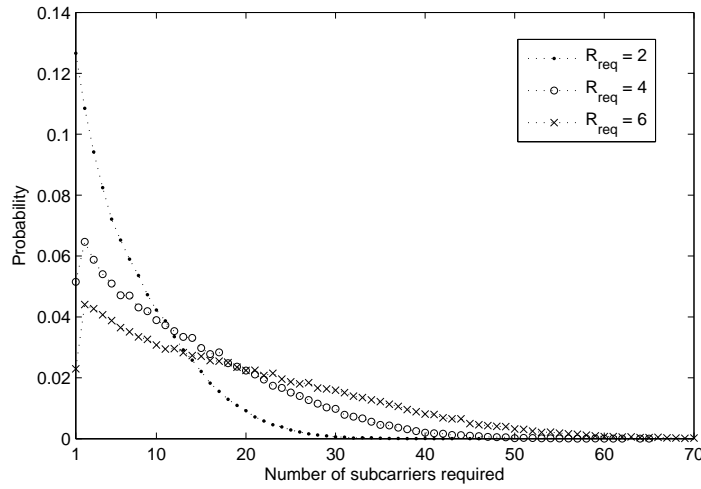
Figure 4.4: Probability distribution $f_n[n_{\mathrm{req}}]$ of the number of subcarriers required by an incoming call for the rate requirement $R_{\mathrm{req}} = 2, 4$ and 6 bits/sec/Hz
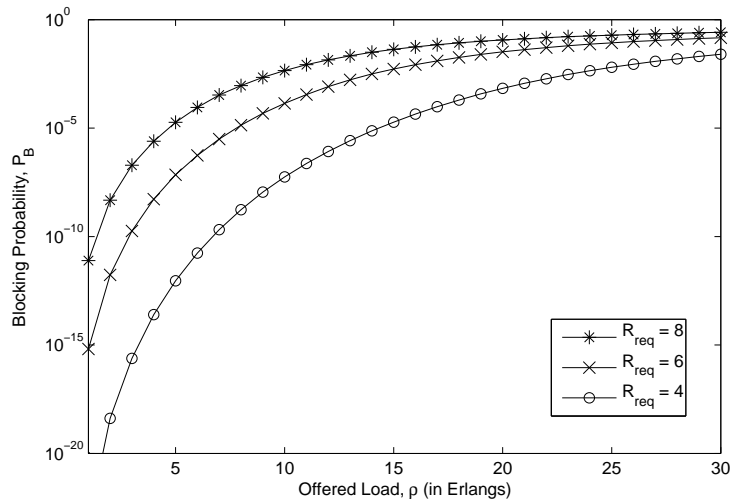
Figure 4.5: Blocking probability versus offered load for rate requirement $R_{\mathrm{req}} = 4, 6$ and 8 bits/sec/Hz

load ρ as shown in Fig. 4.5. We observe that blocking probability increases with R_{req}. This is because, for a higher value of R_{req}, users need more subcarriers on an average and hence experience a higher blocking probability. In Fig. 4.6, we plot the Erlang capacity as a function of R_{req} for 2% and 5% blocking probabilities. This capacity is evaluated by determining the offered load corresponding to $P_B = 2\%$ and 5% in Fig. 4.5. In Fig. 4.7 and Fig. 4.8, we present similar results for fixed $R_{\mathrm{req}} = 4$ bits/sec/Hz and different values of transmit power P_{tx}. In Fig. 4.7, we observe a decreasing trend in blocking probability for increasing values of P_{tx}. This is because, for a higher value of P_{tx}, users need a smaller
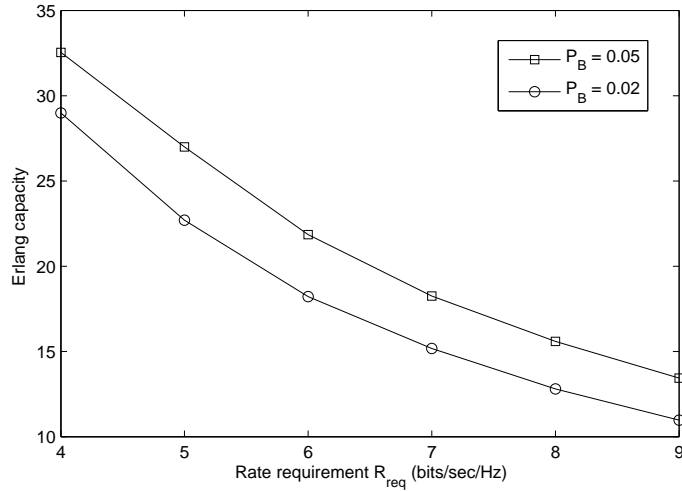
Figure 4.6: Erlang capacity versus rate requirement R_{req} for blocking probability $P_B = 2\%$ and 5%
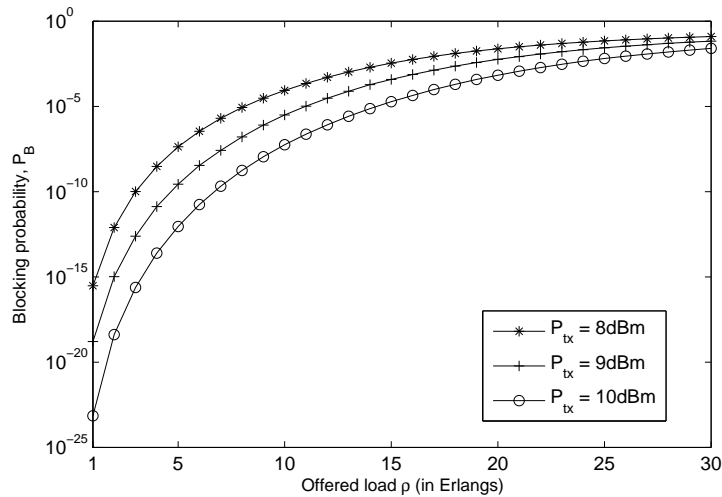
Figure 4.7: Blocking probability versus offered load for BS transmit power per subcarrier $P_{\mathrm{tx}} = 8, 9$ and 10 dBm

number of subcarriers on an average and hence experience a lower blocking probability. In Fig. 4.8, we plot the Erlang capacity as a function of P_{tx} for 2% and 5% blocking probabilities.

4.4.3   Erlang Capacity with relays

In this section we present the numerical results for the Erlang capacity of a relay-assisted cellular system, as described in Section 4.3. In addition to the parameters in Table 4.1 we define system parameters for cellular relays in Table 4.2. For a given offered load, we
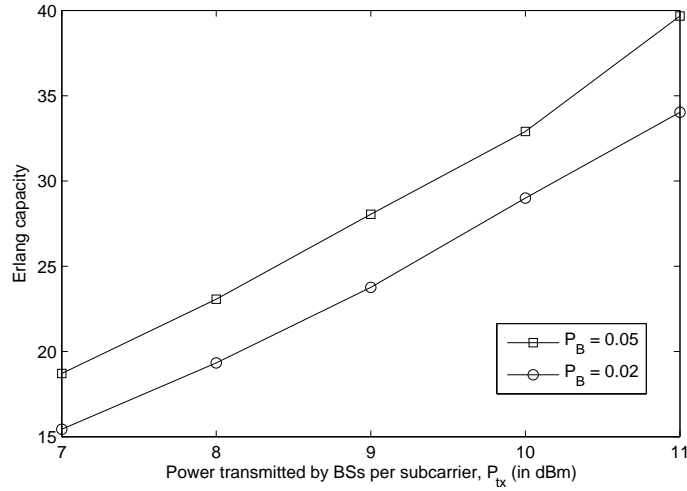
Figure 4.8: Erlang capacity versus BS transmit power per subcarrier P_{tx} for blocking probability $P_B = 2\%$ and 5%
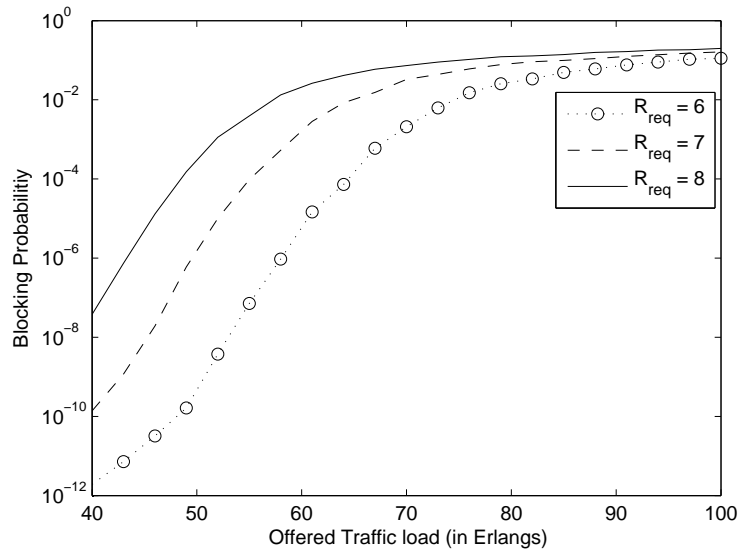
Figure 4.9: Blocking probability versus offered traffic load in Erlangs for different required data rates $R_{req} = 6, 7, 8$ bits/sec/Hz

obtain the probability distributions on the number of subcarriers required on the BS-RS, RS-MS and BS-MS links. Then using the approach described in Section 4.3, we determine the blocking probability of the system.

Fig. 4.9 is a plot of the blocking probability versus offered traffic load in Erlangs, for different values of required data rate R_{req}. We observe that blocking probability decreases with increasing R_{req}. We also observe that blocking probability is much lower than the case without relays, thus demonstrating that introduction of RSs indeed improves the cell capacity.
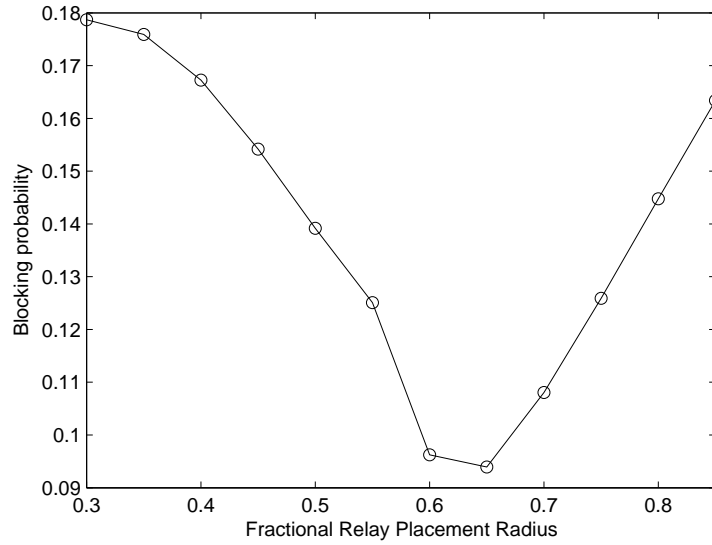
Figure 4.10: Blocking probability versus RS placement radius for offered load $\rho = 100$ Erlangs in the cell
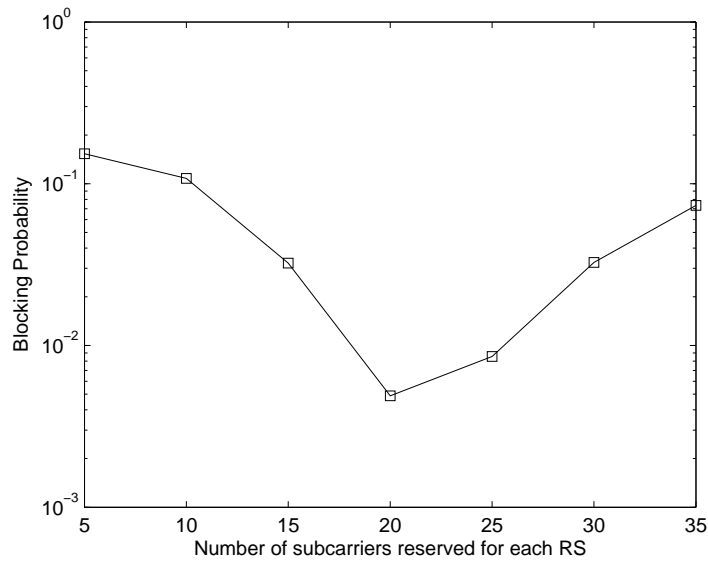
Figure 4.11: Blocking probability versus N_{RS}, the number of subcarriers reserved for each RS for offered load $\rho = 100$ Erlangs in the cell

In Fig. 4.10, we plot the blocking probability versus the fractional RS placement radius for an offered load of 100 Erlangs. The total blocking probability varies because the fraction of calls served directly by the BS and via RS, and the individual blocking probability for these two classes varies with the RS placement radius. The blocking probability is minimum for a RS placement radius of $0.65R$. Thus, this is the optimal radial location for placing the RSs.

We have divided the total number of subcarriers available in the cell, N_{cell} into disjoint sets of N_{RS} for each RS. In Fig. 4.11 we plot the blocking probability versus N_{RS}, the number of subcarriers reserved for each RS. Initially, for a low value of N_{RS}, the blocking probability is high since the subcarriers reserved are insufficient to serve the Type II calls, which are served via RS. On increasing N_{RS}, the blocking probability of Type II calls decreases, hence reducing the overall call blocking probability. As the number of subcarriers reserved for each RS increases further, the number of subcarriers available for the BS decreases. Due to this, there is an increase in the blocking probability of Type I calls, the overall blocking probability increases again. The blocking probability is minimum when $N_{RS} = 20$ subcarriers are reserved for each RS, and the remaining $N_{BS} = 512 - 6 \times 20 = 392$ subcarriers are reserved for the BS's downlink transmissions.

Table 4.2:

SYSTEM PARAMETERS	
Number of Subcarriers available in each cell	$N_{cell} = 512$
Number of subcarriers reserved for each RS	$N_{RS} = 40$
Number of RSs in each cell	$M = 6$
RS placement radius	$\frac{3}{4}R$
Rate requirement of each call	$R_{req} = 6$ bits/sec/Hz
Offered traffic load in Erlangs	$\rho = 100$
Power transmitted by RS per subcarrier	$P_{\text{tx}} = 6$ dBm
MS association power	$\Delta P = -10dB$
BS-RS Shadowing standard deviation	$\sigma_{br} = 3$ dB
RS-MS Shadowing standard deviation	$\sigma_{rm} = 5$ dB
BS-MS Shadowing standard deviation	$\sigma_{bm} = 8$ dB

4.5 Conclusions

In this chapter, we have determined the downlink Erlang capacity of a cellular OFDMA system with 1:1 frequency reuse. The key idea of the approach is to divide incoming calls into classes according to their subcarrier requirement. Arrival rates of these classes have

been obtained from the probability distribution of the number of subcarriers required by users. The system is then modeled as a multi-dimensional Markov chain and techniques used to solve the analogous stochastic knapsack problem are applied to simplify the computation of the blocking probability. We then extend this analysis to a relay-assisted cellular system, obtain numerical results for the optimal RS location and BS-RS subcarrier distribution to achieve maximum Erlang capacity.

We have evaluated the worst case Erlang capacity under the assumption that the alloted subcarriers are used by the MS for the entire call duration. However if voice activity factor is taken into account, the inter-cell interference will be reduced, thus causing an increase in the Erlang capacity of the system. This could be a possible avenue for future investigations. Another research direction could be to determine the capacity for different subcarrier allocation algorithm other than the random allocation scheme considered in this work.

Chapter 5

Packet Loss Analysis of Relay ARQ

5.1 Introduction

In Chapter 2, we have discussed that traditional multi-hop ARQ protocols - hop-by-hop and end-to-end ARQ. We have demonstrated a problem of gross packet loss that will occur when hop-by-hop ARQ is employed in relay-assisted cellular networks. In this section, we propose a simple channel and handover model, which is used to quantify this packet loss during handover. Then we propose modifications to hop-by-hop, and develop two ARQ protocols - Staggered ARQ and Advanced ARQ. The proposed protocols reduce packet loss during handover at the cost of additional queueing delay and signalling overhead respectively. In particular, we show that the staggered ARQ protocol reduces the packet loss during handover and also reduces the total packet delay. The numerical results presented in this chapter are useful in designing the size of the buffer size at a cellular RS. The analysis of packet loss in hop-by-hop ARQ and the proposal of advanced ARQ protocol are collaborative work and are also included in [36].

The rest of the chapter is organized as follows. In Section 5.2, we present a novel channel and handover model which is used to theoretically determine the packet loss during handover. Analysis of packet loss in hop-by-hop ARQ is presented in Section 5.3. Modifications to hop-by-hop ARQ are proposed in Section 5.4 and compared with the performance of hop-by-hop ARQ. In section 5.5, a comparative packet delay analysis of hop-by-hop, end-to-end and the proposed protocols is performed. Section 5.7 summarizes the results and gives directions for extension of this work.

5.2   Channel and Handover Model

We consider a single cell scenario with downlink packet transmission from the BS to an MS via RS. For our analysis, we assume a time-slotted system. In each time slot, the wireless channel can be either in the *good* or *bad* state. In good state, any transmitted packet is received successfully and in bad state the packet is received in error and discarded. The BS-RS link will be referred to as the relay link, and the access link as the access link. We assume a stop-and-wait packet transmission protocol where in every time slot, one packet each is transmitted on the relay and the access links. The relay link channel state is modeled as a Bernoulli independent and identically distributed (i.i.d) random variable across slots, with probability p_g of being in good state and probability $p_b = 1 - p_g$ of being in bad state. Since the BS and RS are stationary, an i.i.d relay channel is a reasonable assumption. We further assume that the relay link and access link channels are independent.

Our objective in this chapter is to determine the packet loss during handover. For this, we need to evaluate the queue length at the RS at the time of handover. However, this is difficult to determine since handover occurs when the signal to noise ratio (SNR) of an MS falls below a threshold for sufficient time. This in turn depends upon the channel condition and the speed of the mobile.

We make a simplifying assumption that if an MS experiences a bad access channel for N consecutive time slots then an inter-RS handover is executed. Further, we assume that a target RS with good access channel is always available for handover. Let p_1 and p_2 be the good-to-bad and bad-to-good transition probabilities of the channel, and $1 - p_1$ and $1 - p_2$ be the transition probabilities of remaining in good and bad states respectively. The access link state is modeled by a discrete time Markov chain as shown in Fig. 5.1, where state 0 corresponds to good channel state and state j (for $j \in [1, N]$) indicates that
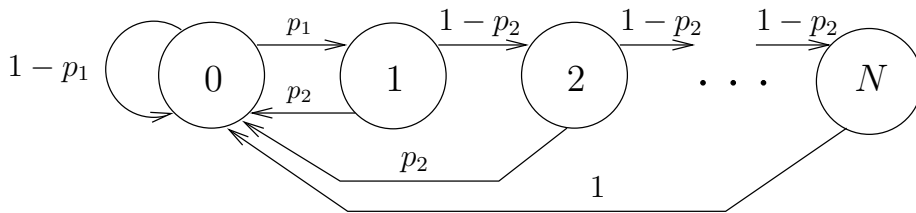

Figure 5.1: Channel and handover model for the RS-MS link

the access channel has been in bad state for j consecutive slots. If the access link is in state j (for $j \in [1, N)$), it can return to state 0 with probability p_2 or it can move to state $j + 1$ with probability $1 - p_2$. When the channel reaches state N, a handover is executed, and due to our assumption of target RS being always available, the system returns to state 0 with probability 1.

As already explained, we consider a single cell scenario with downlink packet transmission from the BS to an MS via RS. We assume that the BS always has a packet to transmit. We assume that acknowledgements (ACKs) and negative acknowledgements (NACKs) to the transmitted packets are always received without error. We consider that the buffer at the RS can hold a maximum of M packets. When the buffer is full, the ARQ can signal this to the BS by delaying the ACKs, thus avoiding further queue build-up. Each time slot is divided into four mini slots, first for an RS to MS packet transmission, followed by an ACK/NACK slot in which the MS sends an ACK to RS if the packet was successfully received, and a NACK otherwise. In the third mini slot, the RS sends an ACK or NACK for the packet received from BS in the previous time slot. If the buffer at the RS already full with M packets, the RS does not send an ACK to BS even if the packet has been successfully received. In this case, the BS does not transmit any packet in the fourth mini slot and waits for an ACK or NACK. If an ACK or NACK is received in the third mini slot, the BS sends a new packet or retransmits the previous packet to the RS in the fourth mini slot[1]. In hop-by-hop ARQ, the packets queued at the RS are lost during inter-RS handover. By employing this mechanism of RS delaying ACKs to BS, there is no packet loss due to buffer overflow at RS and the only cause of packet loss is handover.

5.3 Packet Loss Analysis of Hop-by-Hop ARQ

We determine the probability distribution of queue length at the RS at the time of handover (i.e when the access channel is in state N), and consequently compute the packet loss during handover. We define the state of the system to be (i, j), where i is the queue

---

[1]Though we focus on a specific RS-MS link and do not consider multiple MSs, the analysis remains unchanged if these MSs are scheduled by BS and RS using a round robin scheduler. In this case, consecutive time slots in our analysis correspond to the scheduled slots for an MS.
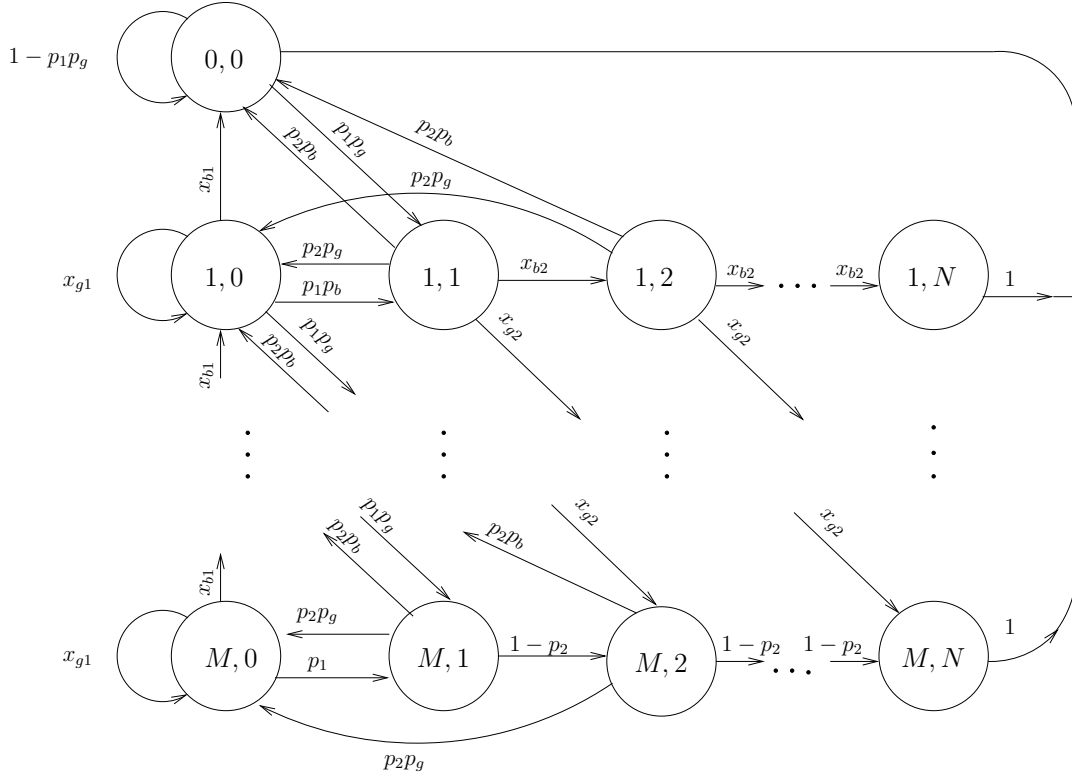
Figure 5.2: Markov chain for analysis of packet loss. For state (i, j), i is the queue length at RS and j is the number of consecutive bad states of RS-MS link

length at the serving RS and j corresponds to state j of the access channel model described in Section 5.2 (i.e the number of consecutive bad states of the access link). This system state evolution can be depicted by the discrete time Markov chain as shown in Fig. 5.2.

The state transition probabilities are given in (5.1-5.12) where $P_{k,l|i,j}$ denotes the transition probability from state (i, j) to state (k, l). After one time slot, the queue length i at RS increases by 1 if the transmission from BS to RS succeeds and that from RS to MS fails. This occurs when the relay link is in good state (with probability p_g) and access link moves from bad state j to state $j+1$ in Fig. 5.1 (with probability p_1 for $j = 0$ and probability $1 - p_2$ for $j \in [1, N)$). This explains the transition probabilities (5.1-5.2). In (5.3-5.4), the queue length i at the RS decreases by one because the relay link is in bad state and access link in good state. Similarly, if both the links are in good or bad states, we obtain the transition probabilities (5.5-5.11). When handover is executed in state (i, N) for $i \in [1, M]$, the i packets queued at the serving RS are lost and the target RS starts with zero queue length. Since the target RS is assumed to have a good channel to the MS after handover, the access channel state moves to state 0 with probability 1.

This explains the transition probability in (5.12).

$$P_{i+1,j+1|i,j} = (1 - p_2)p_g \triangleq x_{g2}, \ i \in [1, M), j \in [1, N) \tag{5.1}$$

$$P_{i+1,1|i,0} = p_1 p_g, \ i \in [0, M), \tag{5.2}$$

$$P_{i-1,0|i,j} = p_2 p_b, \ i \in [1, M], \ j \in [1, N), \tag{5.3}$$

$$P_{i-1,0|i,0} = (1 - p_1)p_b, \triangleq x_{b1} \ i \in [1, M], \tag{5.4}$$

$$P_{i,j+1|i,j} = (1 - p_2)p_b \triangleq x_{b2}, \ i \in [1, M), \ j \in [1, N) \tag{5.5}$$

$$P_{i,0|i,j} = p_2 p_g, \ i \in [1, M], \ j \in [1, N), \tag{5.6}$$

$$P_{i,0|i,0} = (1 - p_1)p_g \triangleq x_{g1}, \ i \in [1, M), \tag{5.7}$$

$$P_{i,1|i,0} = p_1 p_b, \ i \in [0, M], \tag{5.8}$$

$$P_{0,0|0,0} = 1 - p_1 p_g, \tag{5.9}$$

$$P_{M,1|M,0} = p_1, \tag{5.10}$$

$$P_{M,j+1|M,j} = (1 - p_2) \ j \in [1, N), \tag{5.11}$$

$$P_{0,0|i,N} = 1, \ i \in [1, M]. \tag{5.12}$$

Let the steady state probability of state (i, j) be denoted as $\pi_{i,j}$. The corresponding balance equations are as follows,

$$p_1 p_g \pi_{0,0} = x_{b1}\pi_{1,0} + p_2 p_b \sum_{j=1}^{N-1} \pi_{1,j} + + \sum_{i=1}^{M} \pi_{i.N}, \tag{5.13}$$

$$\pi_{i,1} = p_1 p_g \pi_{i-1,0} + p_1 p_b \pi_{i,0} \quad i \in [1, M), \tag{5.14}$$

$$\pi_{i,j} = x_{g2}\pi_{i-1,j-1} + x_{b2}\pi_{i,j-1}, \ i \in [2, M), \ j \in [1, N], \tag{5.15}$$

$$\pi_{1,j} = x_{b2}\pi_{1,j-1}, \ j \in [2, N], \tag{5.16}$$

$$(1 - x_{g1})\pi_{i,0} = x_{b1}\pi_{i+1,0} + p_2 p_g \sum_{j=1}^{N-1} \pi_{i,j} + p_2 p_b \sum_{j=1}^{N-1} \pi_{i+1,j}, \ i \in [1, M), \tag{5.17}$$

$$(1 - x_{g1})\pi_{M,0} = p_2 p_g \sum_{j=1}^{N-1} \pi_{M,j}, \tag{5.18}$$

$$\pi_{M,1} = p_1 p_g \pi_{M-1,0} + p_1 \pi_{M,0}, \tag{5.19}$$

$$\pi_{M,j} = x_{g2}\pi_{M-1,j-1} + (1 - p_2)\pi_{M,j-1}, \ j \in [2, N]. \tag{5.20}$$

$$1 = \sum_{i=0}^{M} \sum_{j=0}^{N} \pi_{i,j} + \pi_{0,0} \tag{5.21}$$

We express the steady state probability of each state as a linear combination of the probabilities $\pi_{i,0}$ for $i \in [0, M]$. This set of simultaneous equations in $\pi_{i,0}$ can then be solved to obtain all $\pi_{i,j}$. The steps followed in the derivation are that, we first express each $\pi_{i,j}$ as a linear combination of $\pi_{k,1}$ with k going from 0 to i, and then, using (5.14) we express each $\pi_{k,1}$'s in terms of the $\pi_{k,0}$ probabilities. For $i = 1$ and $i = 2$, we have,

$$
\begin{aligned}
\pi_{1,j} &= x_{b2}\pi_{1,j-1} \quad 2 \le j \le N \\
&= x_{b2}^{j-1}\pi_{1,1} \\
&= x_{b2}^{j-1}(p_1 p_g \pi_{0,0} + p_1 p_b \pi_{1,0}) \quad j \in [1, N]
\end{aligned}
$$
(5.22)
(5.23)

$$
\begin{aligned}
\pi_{2,j} &= x_{g2}\pi_{1,j-1} + x_{b2}\pi_{2,j-1} \quad j \in [1, N] \\
&= x_{g2}x_{b2}^{j-2}(p_1 p_g \pi_{0,0} + p_1 p_b \pi_{1,0}) + x_{b2}\pi_{2,j-1} \quad j \in [2, N]
\end{aligned}
$$
(5.24)

By induction on j we have,

$$
\pi_{2,j} = (j-1)x_{g2}x_{b2}^{j-2}p_1 p_g \pi_{0,0} + [(j-1)x_{g2}x_{b2}^{j-1}p_1 p_b + x_{b2}^{j-1}p_1 p_g]\pi_{1,0} + x_{b2}^{j-1}p_1 p_b \pi_{2,0} \quad (5.25)
$$

Further, by applying induction on i we get,

$$
\pi_{i,j} = {}^{j-1}C_{i-h}x_{g2}^{i-1}x_{b2}^{j-i}p_1 p_g \pi_{0,0} + \sum_{h=1}^{i}\left({}^{j-1}C_{i-h}x_{g2}^{i-h}x_{b2}^{j-i+h-1}p_1 p_b + {}^{j-1}C_{i-h-1}x_{g2}^{i-h-1}x_{b2}^{j-i+h}p_1 p_g \right)\pi_{h,0}
$$

$$
i \in [1, M), j \in [1, N] \tag{5.26}
$$

where,

$$
{}^{n}C_k = \begin{cases} \frac{n!k!}{(n-k)!} & \text{if } n, k, n-k \ge 0 \\ 0 & \text{otherwise} \end{cases}
$$

Using (5.26) and solving for $\pi_{i,0}$, we evaluate the steady state probabilities of all states. Since the handover occurs when the channel is in state (i, N) for all $i \in [0, M]$, the probability of handover can be expressed as $p_{HO} = \sum_{i=0}^{M} \pi_{i,N}$. Accordingly, the average queue length at the time of handover is given by $q_{HO} = \frac{1}{p_{HO}} \sum_{i=0}^{M} i\pi_{i,N}$. Note that the average queue length at the time of handover corresponds to the number of packets lost every time a handover occurs. The product of the average queue length and the probability of handover, $q_{HO}.p_{HO}$, corresponds to the average packet loss per slot.

5.4 Proposed modifications to Hop-by-hop ARQ

In this section, we propose modifications to hop-by-hop ARQ in order to reduce the packet loss during handover. We propose two new protocols, 'Staggered ARQ' and 'Advanced ARQ'. Comparison of the performance of these protocols with hop-by-hop ARQ is presented in Section 5.6.

5.4.1 Staggered ARQ Protocol

We have noted that the MS hands over to another RS after N consecutive bad slots of the access link. All the packets queued at the RS are lost at the time of handover. We propose that the RS shall delay the sending of ACKs to the BS after the access link experiences N_1 consecutive bad slots, where $N_1 < N$. Thus, further packet transmissions from BS to RS will be suspended or staggered, thus preventing excessive queue buildup at RS. If a good channel state is now encountered on the access link, the RS transmits the delayed ACK to the BS, and the packet transmission from BS to RS is resumed. On the other hand, if $N_2 = N - N_1$ more bad states are encountered on the access link, the MS hands over to another RS.

Due of the staggering mechanism, fewer packets are queued at the RS at the time of handover and hence the packet loss is reduced. We prove this by analytically determining the average queue length at the RS and the probability of handover as done for the case of hop-by-hop ARQ in Section 5.3. Fig. 5.3 shows the Markov chain for the analysis of staggered ARQ protocol. The BS stops transmitting packets to the RS after N_1 bad states of the access link. Thus, unlike the hop-by-hop ARQ protocol in Fig. 5.2, we do not have state transitions i, j to $i+1, j+1$ for $j \geq N_1$. If the access link experiences $N_2 = N - N_1$ more bad states, the MS is handed over to another RS. Thus, the states $(i, N_1 + N_2)$ for all $i \in [1, M]$ transition to state $(0, 0)$ with probability 1.

5.4.2 Advanced ARQ protocol

In this scheme, the RS forwards ACK/NACK from the MS to the BS in addition to its own ARQ feedback. To avoid the packet loss during handover, the BS maintains two pointers for the ARQ states of the relay link and the access link as shown in Fig. 5.4. The BS clears a packet from its transmit buffer after it is successfully received at the MS.
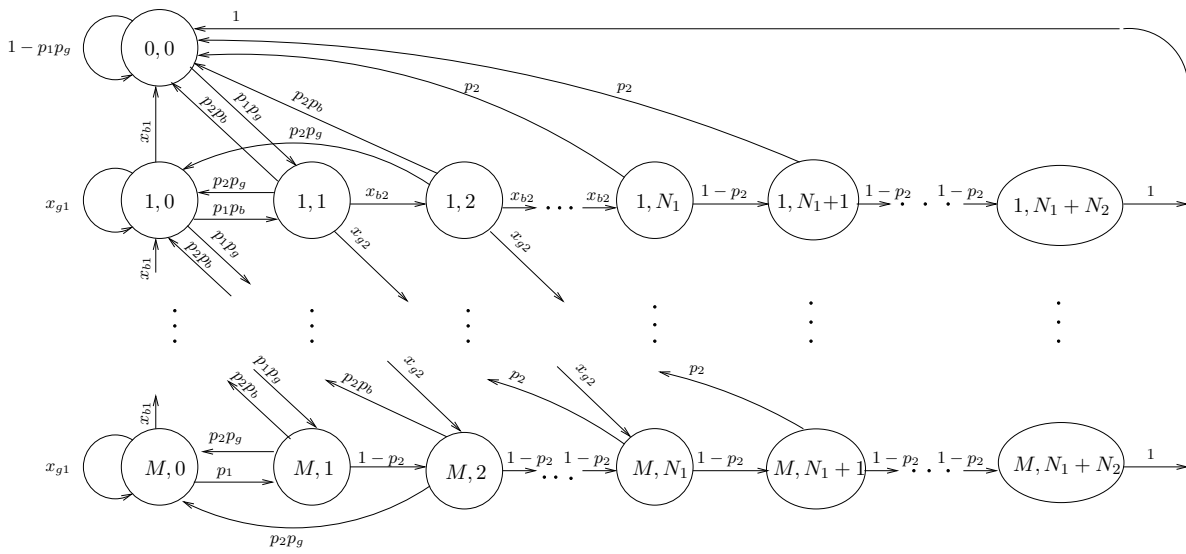
Figure 5.3: Markov chain for analysis of packet loss of staggered ARQ. For state (i,j), i is the queue length at RS and j is the number of consecutive bad states of the access link. BS stops transmitting packets to the RS after N_1 bad states of the access link
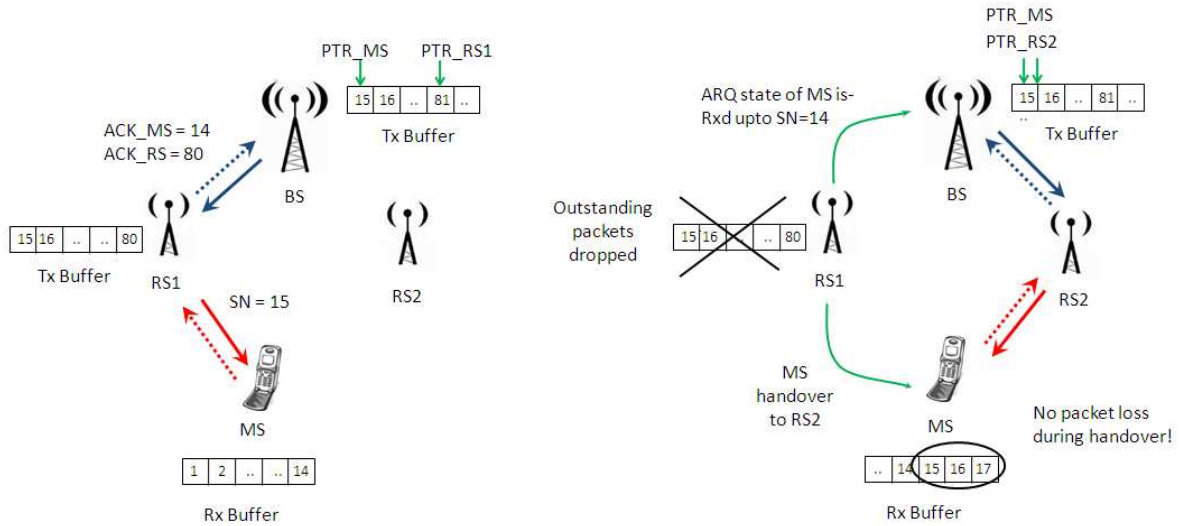
Figure 5.4: Illustration of how packet loss during handover is averted by the use of the Advanced ARQ protocol

Thus, at the time of handover, the packet queued at the relay is also present in the BS's buffer. The BS just needs to set its new relay link pointer equal to the access link ARQ pointer. Thus, advanced ARQ ensures seamless handover without any packet loss.

5.5 Packet Delay Analysis

In Section 5.4 we proposed the staggered and advanced ARQ protocols, which reduce the packet loss in hop-by-hop ARQ, at the cost of additional queueing delay and signalling overhead respectively. In this section we compare the total packet delays of these protocols and compare them with hop-by-hop ARQ.

Note that we compute the packet delay from the time the packet is at the head-of-the-queue at the BS, till it is successfully received by the MS, via the RS. For all the three protocols, the packet delay comprises of the transmission time of packets and ACKs, queueing delay at BS due to a full buffer at RS, and queueing delay at RS. In Section 5.2, we assume that the RS stops sending ACKs to the BS when the RS buffer is full. Thus, packets experience a queueing delay at the BS. For the staggered ARQ protocol, packets experience an additional queueing delay at BS since the BS stops packet transmission to the RS after N_1 bad states occur on the access link.

5.5.1 Queueing Delay at BS due to full RS Buffer

As described in Section 5.2, we assume each time slot consists of four mini-slots, the first for RS-MS data transmission, second for ACK/NACK from MS to RS, third for ACK/NACK from RS to BS and the fourth mini slot for BS-RS transmission. If the buffer at the RS is full, the RS stops sending ACKs to the BS, thus preventing further packet transmissions from BS to RS. The next packet is queued at the BS until space is created in the RS buffer by a successful RS-MS transmission. After a successful RS-MS transmission, the RS sends the delayed ACK to the BS, and the packet queued at the BS is transmitted to RS. We compute the average queueing delay at BS in terms of the number of slots a packet is queued at BS while the RS buffer is full.

We first compute the queueing delay in case of the hop-by-hop ARQ protocol. By using the transition probabilities in Fig. 5.2, we evaluate the probability q_i of a queueing delay of i slots occurring before the packet is transmitted, and take an expectation over i to determine the average queueing delay $\sum_{i=1}^{N} i.q_i$. A queueing delay of i slots occurs when the following series of events occur,

1. The system transitions to the buffer full state because of a good BS-RS link and bad access link.

2. If the bad access link state persists for the next i time slots. Thus, since the buffer remains full, the RS does not send an ACK for the packet received through the good relay link in order to avoid buffer overflow. Thus, the packet is delayed in the queue at BS for i slots.

3. The RS-MS link returns to good state in the next time slot, creating space in the buffer. Now the RS sends the delayed ACK to the BS, and waiting period of the packet queued at the BS ends.

For example, a queueing delay of 1 slot occurs when the system is initially in state $(M-1, j)$ for $j \in [0, N-2]$ and it moves to the buffer full state (M, j) for $j \in [1, N-1]$. The probability of this transition is x_{g2}. The bad access link persists in the next time slot with probability $(1-p_2)$ and the system moves from (M, j) to $(M, j+1)$ for $j \in [1, N-1]$. The waiting period of the packet in the queue at BS ends when access link returns to good state. This is a transition from (M, j) to $(M, 0)$ with probability $p_2 p_g$ or to $(M-1, 0)$ with probability $p_2 p_b$, for $j \in [1, N-1]$. If the system is in state (M, N), the waiting period of the packet ends when the MS hands over to another RS with probability 1.

A queueing delay of 1 slot can also occur if the system is initially in state $(M, 0)$. With probability p_1, the access link moves to bad state $(M, 1)$ in the next time slot, the RS delays its ACK to the BS and the packet queued at BS experiences experiences a delay of one slot. Thus, the probability q_1 of a queueing delay of 1 slot is the sum of probabilities of entering state (M, j) for $j \in [0, N-1]$, and the subsequent events occur as described above.

$$q_1 = \pi_{M,0} p_1 p_2 + p_1 p_g \pi_{M-1,0}(1-p_2)p_2 + x_{g2} \sum_{j=1}^{N-3} \pi_{M-1,j}(1-p_2)p_2 + x_{g2}\pi_{M-1,N-2}(1-p_2).1$$

$$= p_1 p_2 \pi_{M,0} + p_1 p_g (1-p_2)p_2 \pi_{M-1,0} + x_{g2}(1-p_2) \left(\sum_{j=1}^{N-3} \pi_{M-1,j} p_2 + \pi_{M-1,N-2} \right) \quad (5.27)$$

Similarly we compute the probability of a queueing delay of i slots for $i \in [1, N]$. Generalizing (5.27), a queueing delay of i slots for $i \in [1, N]$ occurs when the system enters one of the buffer full state (M, j) for $j \in [1, N-i]$, followed by i bad RS-MS link slots, and then a good RS-MS link state, thus ending the waiting period. Note that the maximum queueing delay is N slots. This corresponds to being in state $(M, 0)$ initially, and the RS-MS link experiencing bad channel state for N consecutive time slots after which a

handover takes place and ends the waiting period of the packet.

$$
q_i = \begin{cases}
p_1(1-p_2)^{i-1}p_2\pi_{M,0} + p_1p_g(1-p_2)^i p_2\pi_{M-1,0} + x_{g2}(1-p_2)^i p_2\sum_{j=1}^{N-i-2}\pi_{M-1,j} \\
\quad + x_{g2}(1-p_2)^i\pi_{M-1,N-i-1}, \quad i \in [1, N-3] \\
p_1(1-p_2)^{N-3}p_2\pi_{M,0} + p_1p_g(1-p_2)^{N-2}p_2\pi_{M-1,0} + x_{g2}(1-p_2)^{N-2}\pi_{M-1,1} \quad i = N-2 \\
p_1(1-p_2)^{N-2}p_2\pi_{M,0} + p_1p_g(1-p_2)^{N-1}\pi_{M-1,0} \qquad\qquad\qquad\quad i = N-1 \\
p_1(1-p_2)^{N-1}\pi_{M,0} \qquad\qquad\qquad\qquad\qquad\qquad\qquad\quad i = N
\end{cases}
$$

The expected queueing delay due to RS buffer being full, for every packet transmission is, $D_b^{hbh} = \sum_{i=1}^N i.q_i$. The queueing delay in the advanced ARQ protocol proposed in Section 5.4 is equal to the delay D_b^{hbh} in the case of hop-by-hop ARQ. However, the delay analysis of hop-by-hop ARQ is not applicable to the staggered ARQ protocol, because unlike hop-by-hop ARQ, there are no $(M-1, j-1)$ to (M, j) transitions for $j > N_1$ in the staggered ARQ protocol. Using the transition probabilities in Fig. 5.3, we compute the probability of a queueing delay of i slots as,

$$
q_i = \begin{cases}
p_1(1-p_2)^{i-1}p_2\pi_{M,0} + p_1p_g(1-p_2)^i p_2\pi_{M-1,0} + x_{g2}(1-p_2)^i p_2\sum_{j=1}^{N_1-2}\pi_{M-1,j}, \quad i \in [1, N_2] \\
p_1(1-p_2)^{i-1}p_2\pi_{M,0} + p_1p_g(1-p_2)^i p_2\pi_{M-1,0} + x_{g2}(1-p_2)^i p_2\sum_{j=1}^{N-i-2}\pi_{M-1,j} \\
\qquad\qquad + x_{g2}(1-p_2)^i\pi_{M-1,N-i-1}, \qquad\qquad\qquad\qquad i \in [N_2+1, N-1) \\
p_1(1-p_2)^{N-2}p_2\pi_{M,0} + p_1p_g(1-p_2)^{N-1}\pi_{M-1,0}, \qquad\qquad\quad i = N-1 \\
p_1(1-p_2)^{N-1}\pi_{M,0}, \qquad\qquad\qquad\qquad\qquad\qquad\qquad\quad i = N
\end{cases}
$$

The expected queueing delay due to a full RS buffer, in case of staggered ARQ is $D_b^{stg} = \sum_{i=1}^N i.q_i$. The delay D_b^{stg} is expected to be smaller than D_b^{hbh} in staggered ARQ, since the queue length at RS is controlled by staggering BS-RS data transmission, the probability of the RS buffer being full is low.

5.5.2 Additional Queueing Delay at BS in Staggered ARQ

In the staggered ARQ, we reduce packet loss during handover by halting the BS to RS packet transmissions when the access link is bad for $N_1 < N$ consecutive slots. Due to this, packets experience an additional queueing delay at the BS. We determine this delay by evaluating the probabilities of the delay being i slots for $i \in [1, N_2]$ as follows,

$$
q_i = (1-p_2)^i p_2 \sum_{j=1}^{M-1}\pi_{j,N_1}, i \in [1, N_2) \tag{5.28}
$$

$$
q_{N_2} = (1-p_2)^i \pi_{j,N_1} \tag{5.29}
$$

Each q_i is a sum over $k \in [1, M - 1]$ of the probability of entering state (k, N_1) and then encountering i consecutive bad access link states. We do not consider the probability of entering state (M, N_1) because the delay after entering this state has already been taken into account in D_s^{stg}, the queueing delay due to a full RS buffer. Thus, the additional queueing delay due to halt of BS to RS transmission in the staggered ARQ protocol is $D_s^{stg} = \sum_{i=1}^{N_2} i.q_i$.

5.5.3   Total Packet Delay

Now we analytically determine the total delay in successful transmission of a packet from the BS to the MS, and compare the results for the proposed protocols with the hop-by-hop ARQ. Let T be the time of transmission of the packet and kT, the transmission time required for ACK or NACK packet. In other words, k is the ratio of ACK size to the packet size. Assume that ACK/NACK packet are never lost. We assume that packet retransmission takes place only on receipt of NACK and not by due to timeout. The total packet delay is defined as the time from when a packet is at the head of the queue at the BS, till it is successfully received at the MS. It includes the queueing delay at BS due to full RS buffer, queueing delay at RS and the transmission time over the relay and access links. The delay before the packet reaches the head of the BS queue depends on the packet arrival process and the scheduling policy at the BS. We do not consider it for comparison of the packet delay performance of the three protocols considered.

Hop-by-hop ARQ

We determine the analytical expression for the packet delay T_d as the sum of the delay T_r on the relay link, T_a on the access link. T_r includes the queueing delay at the BS D_b^{hbh} for every packet evaluated previously, and T_a includes the queueing delay at the RS. For each link, we evaluate $Pr(i)$, the probability that i packet retransmissions take place and the $(i+1)^{th}$ retransmission is successfully received. The delay on each link is the expectation over i where i is the number of retransmissions. First we evaluate the delay T_r for the relay link. For every retransmission of the packet, an average queueing delay of $D_b^{hbh}.T$

sec occurs. Thus, the delay T_r is,

$$T_r = \sum_{i=0}^{\infty} [(i+1)(T + D_b^{hbh}.T) + ikT]Pr(i)$$

$$= \sum_{i=0}^{\infty} T[(i+1)(1 + D_b^{hbh}) + ik].p_b^i p_g$$

$$= T(1 + D_b^{hbh})\left(1 + \frac{p_b}{p_g}\right) + \frac{kTp_b}{p_g}$$

When a packet is successfully received at the RS, it enters the queue at the RS and is transmitted to the MS after the packets in front of it in the queue are transmitted successufully. Thus, the access link packet delay is the product of the average queue length at the RS and the average transmission time for one packet. The average queue length at the RS is,

$$q_{avg} = \sum_{i=1}^{M} i.\left(\sum_{j=0}^{N} \pi_{i,j}\right) \tag{5.30}$$

Note that this average queue length is different from the q_{HO} computed in Section 5.3 which was the average queue length at the time of handover. q_{HO} depends only on the steady state probabilities $\pi_{i,N}$ for $i \in [1, M]$ while q_{avg} depends on all the steady state probabilities $\pi_{i,j}$ for $i \in [1, M]$ and $j \in [0, N]$.

The average packet transmission time on the access link depends on the number of retransmissions of the packet. We have modelled the access channel state as a Markov chain with good-to-bad transition probability p_1 and bad-to-good transition probability p_2. We have $Pr(i) = Pr(i|G)p_g + Pr(i|B)p_b$ where $Pr(i|G)$ is the conditional probability of i retransmissions when the channel is initially in good state and $Pr(i|B)$, the conditional probability with the channel initially in bad state.

$$Pr(i) = Pr(i|G)p_g + Pr(i|B)p_b$$

$$= p_1(1-p_2)^{i-1}p_2\frac{p_2}{p_1 + p_2} + (1-p_2)^i p_2 \frac{p_1}{p_1 + p_2}$$

$$= \frac{p_1 p_2 (1-p_2)^{i-1}}{p_1 + p_2}$$

There can maximum $N-1$ retransmissions of a packet of the access link, after which the MS will handover to another RS. Thus, the total delay on the access link T_a which is

a product of q_{avg} and the average packet transmission time is,

$$T_a = q_{avg} \sum_{i=0}^{N-1} ((i+1)T + ikT).Pr(i)$$

$$= q_{avg}.\left(T + T(1+k)\frac{p_1 p_2}{p_1 + p_2} \sum_{i=0}^{N-1} i.(1-p_2)^{i-1} \right)$$

$$= q_{avg}.\left(T + \frac{p_1}{p_1 + p_2} T(1+k) \left(\frac{1 - (1-p_2)^N}{p_2} - N(1-p_2)^{N-1} \right) \right)$$

Thus, the total packet delay in the hop-by-hop ARQ protocol is $T_{hbh} = T_a + T_r$. It is the sum of the queueing delay and packet transmission time on the relay and access links.

Staggered ARQ

For the staggered ARQ protocol, the packet delay on the relay link will include the term D_s for the additional queueing delay due to half of BS-RS data transmission when the access link experiences N_1 consecutive bad states. The packet delay on the access link T_a is smaller because the average queue length at the RS, q_{avg} is smaller for staggered ARQ. Thus the total delay T_{stg} is the sum of the packet delays on the relay and access link as follows,

$$T_r = T(1 + D_b^{stg} + D_s^{stg}) \left(1 + \frac{p_b}{p_g} \right) + \frac{kTp_b}{p_g} \tag{5.31}$$

$$T_a = q_{avg}.\left(T + \frac{p_1}{p_1 + p_2} T(1+k) \left(\frac{1 - (1-p_2)^N}{p_2} - N(1-p_2)^{N-1} \right) \right) \tag{5.32}$$

$$T_{stg} = T_r + T_a \tag{5.33}$$

Advanced ARQ

In the proposed Advanced ARQ protocol, the RS forwards the ACK/NACKs received from the MS to the BS. This causes signalling overhead and an increase in the total packet transmission time. The increase on the total transmission time corresponds to the ACK/NACK forwarded by RS to BS for every packet transmission on the access link. We account for this delay by considering that ACKs for double the duration on one ACK, i.e. of duration $2kT$ sec are transmitted by the MS to RS on the access link. This adds to the access link delay T_a. The average queue length at the RS in T_a is same as that in the hop-by-hop ARQ protocol. The packet delay T_r on the relay link is same as in case

of hop-by-hop ARQ. Thus,

$$T_r = T(1 + D_b^{hbh}) \left(1 + \frac{p_b}{p_g}\right) + \frac{kTp_b}{p_g} \tag{5.34}$$

$$T_a = q_{avg} \cdot \left(T + \frac{p_1}{p_1 + p_2} T(1 + 2k) \left(\frac{1 - (1 - p_2)^N}{p_2} - N(1 - p_2)^{N-1}\right)\right) \tag{5.35}$$

$$T_{adv} = T_r + T_a \tag{5.36}$$

5.6 Comparative Numerical Results

| SYSTEM PARAMETERS	
Prob. of relay channel being good	$p_g = 0.8$
Prob. of relay channel being bad	$p_b = 0.2$
Good to bad transition prob. of access channel	$p_1 = 0.3$
Bad to good transition prob. of access channel	$p_2 = 0.3$
Buffer size at relay	$M = 25$ packets
No. of consecutive bad states of access link to trigger handover	$N = 7$
No. of consecutive bad states of access link to stagger BS-RS transmission	$N_1 = 5$
Time slot duration	$T = 1$ msec
Ratio of ACK size to packet size	$k = 1/10$
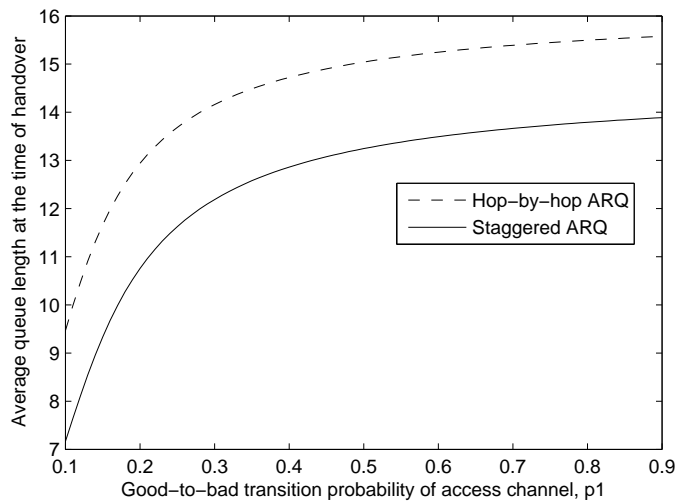
Figure 5.5: Average queue length at RS versus p_1, the good-to-bad transition probability of the access channel
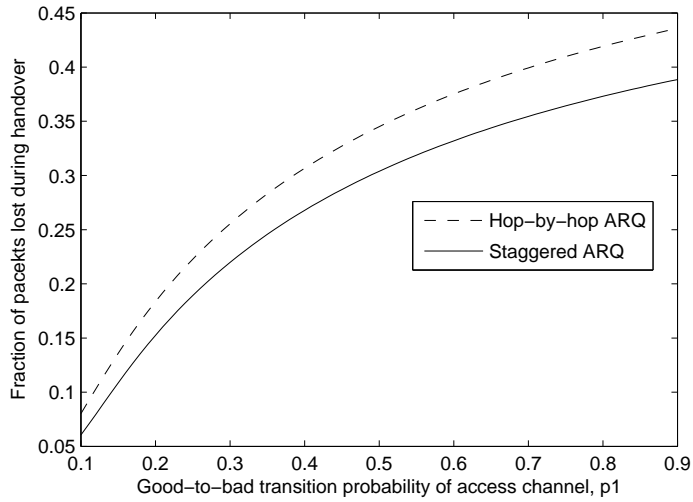
Figure 5.6: Fraction of packets lost due to handover versus p_1, the good-to-bad transition probability of the access channel
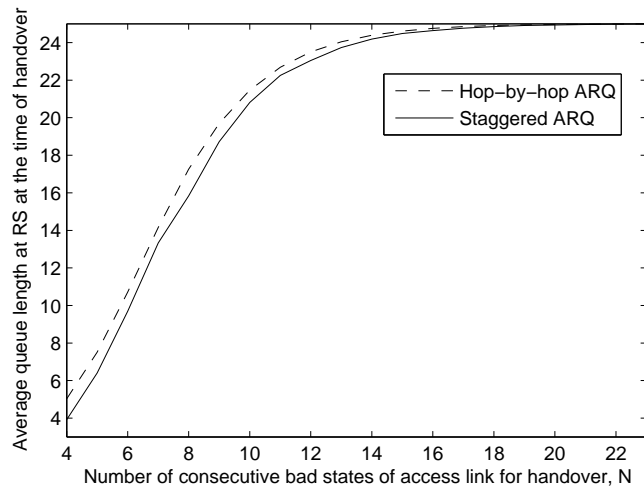

Figure 5.7: Average queue length at RS versus N, the number of consecutive bad slots of the access link after which a handover to another RS occurs

In this section we present numerical results of the packet loss for the proposed staggered ARQ and advanced ARQ protocols and compare them with hop-by-hop ARQ. The advanced ARQ protocol has zero packet loss due to handover but involves additional signalling overhead which adds to the total packet transmission delay. On the other hand, staggered ARQ has non-zero packet loss without signalling overhead, but at the cost of additional queueing delay. The results presented in this section are also useful in designing the buffer size at the RS.

The system parameters chosen for the numerical analysis are as shown in Table I. In Fig. 5.5 we plot the average queue length at the RS versus the good-to-bad transition
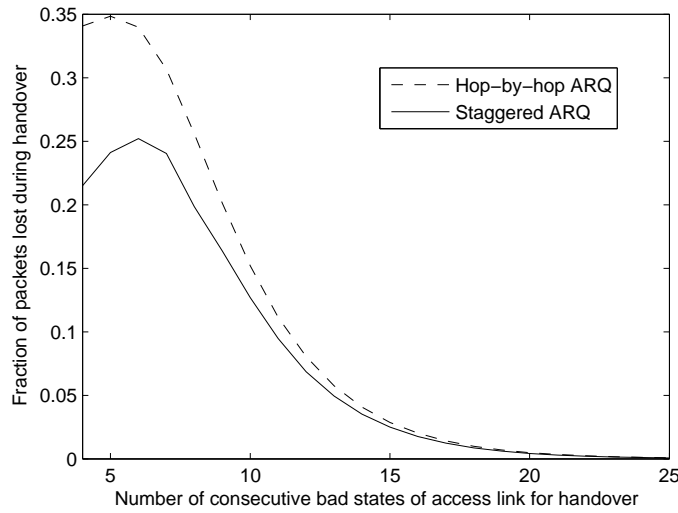
Figure 5.8: Fraction of packets lost due to handover versus N, the number of consecutive bad slots of the access link after which a handover to another RS occurs.
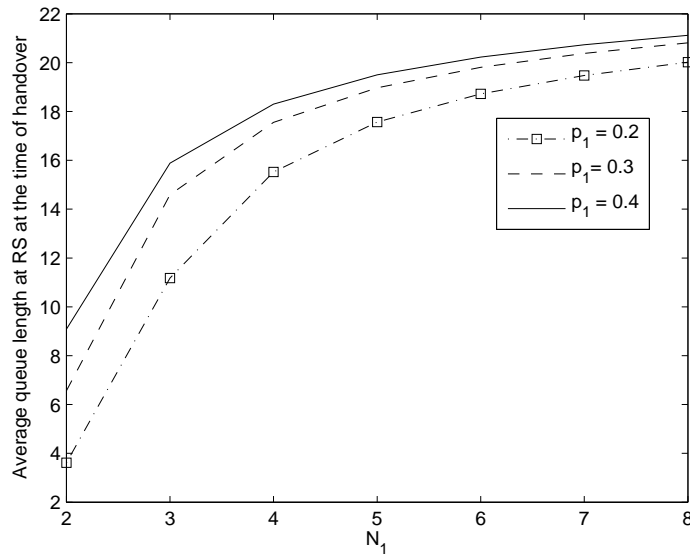

Figure 5.9: Average queue length at RS versus N_1, the number of consecutive bad slots of the access link after which BS-RS transmissions are halted in the staggered ARQ protocol

probability of the access channel, p_1 for hop-by-hop and staggered ARQ. As expected, the queue length increases with p_1. However, the queue length is smaller in case of staggered ARQ. The average queue length q_{HO} multiplied by the probability of handover p_{HO} is equal to the fraction of packets lost due to handover. The variation of this fractional packet loss with p_1 is shown in Fig. 5.6. It is clearly observed that the packet loss is decreased by the use of staggered ARQ, as compared to hop-by-hop ARQ.

Plots of average queue length and packet loss versus N, the number of consecutive
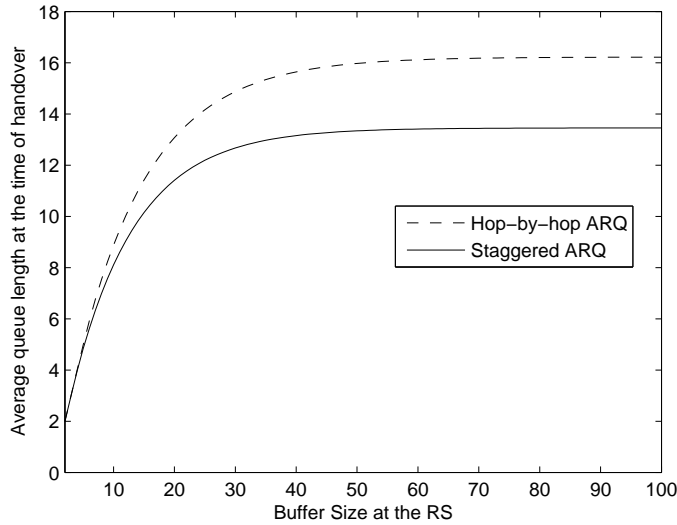
Figure 5.10: Average queue length at RS versus M, the size of the buffer at the RS
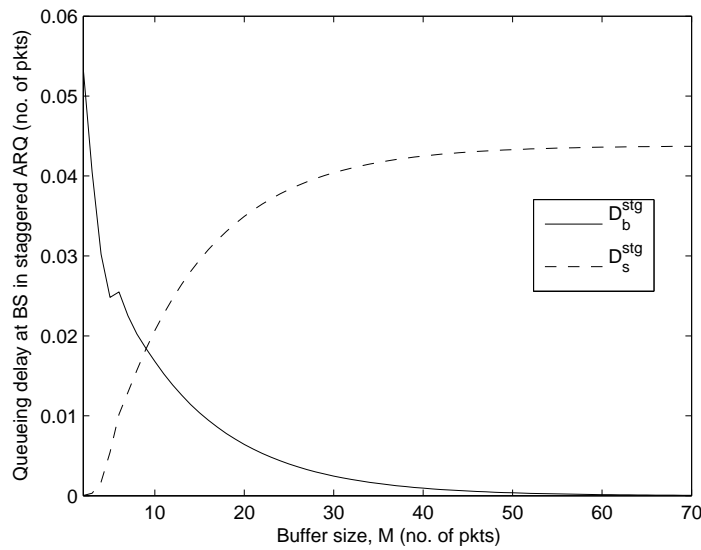

Figure 5.11: Plot of D_b^{stg}, the average queueing delay due to full RS buffer and D_s^{stg}, the average queueing delay due to halt of BS-RS transmissions after N_1 consecutive bad states, versus M, the size of the buffer at the RS

bad states before handover are presented in Fig. 5.7 and Fig. 5.8 respectively. The average queue length q_{HO} decreases The packet loss decreases with increase in N since the handover probability decreases. Fig. 5.9 is a plot of the average queue length versus the factor N_1 in the staggered ARQ protocol, for different values of p_1. N_1 is the number of bad access link states after which the BS stops transmitting packets to the RS. As N_1 increases, the BS stops transmitting packets to the RS after a greater number of bad
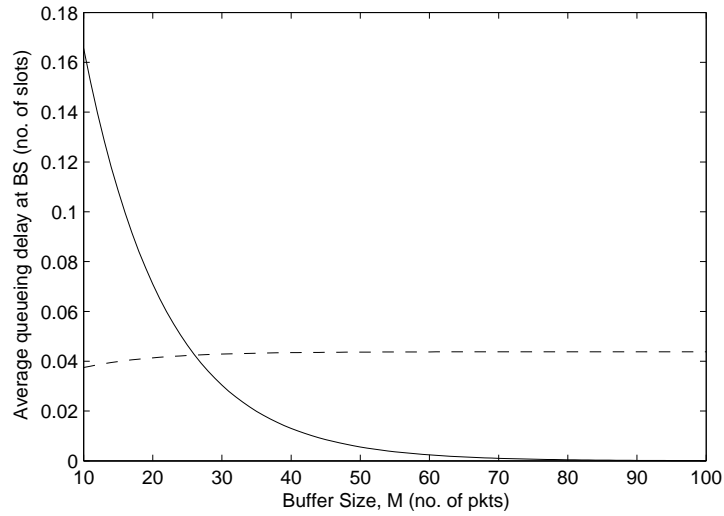
Figure 5.12: Average queueing delay at the BS versus M, the size of the buffer at the RS
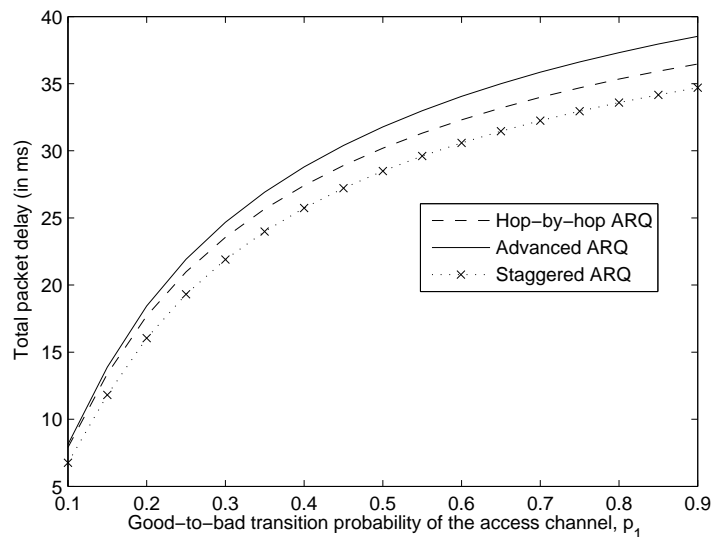
Figure 5.13: Total packet delay versus p_1, the good-to-bad transition probability of the access channel

states of access link. Hence, a greater queue length builds up at the RS for a higher value of N_1.

Now we study the variation of average queue length at the time of handover, q_{HO} with the RS buffer size M. As described in Section 5.2, we assume that there is no packet loss due to buffer overflow because the RS stops sending ACKs to the BS in the buffer is full. In this case, the packets will suffer an additional queueing delay at the BS. A larger buffer size implies lesser queuing delay, but greater queue length building up at the RS, and hence higher the packet loss due to handover. Fig. 5.10 is a plot of the average queue

Figure 5.14: Total packet delay versus buffer size at RS, M

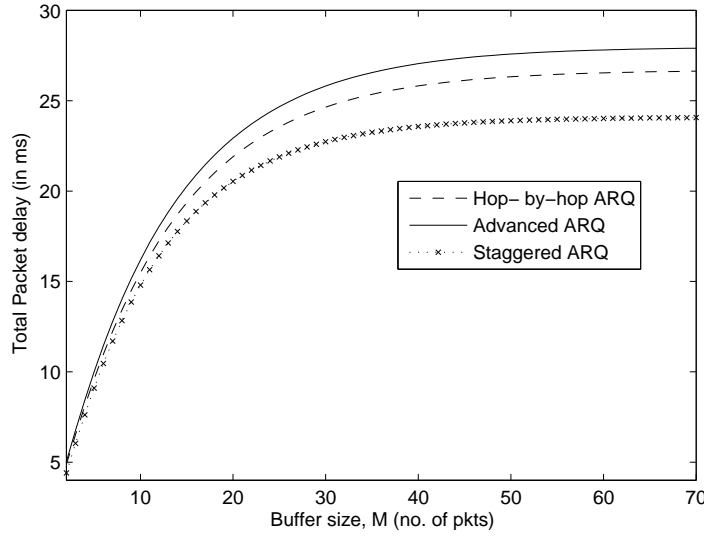length q_{HO} versus the buffer size M. For hop-by-hop ARQ, the queue length saturates to a constant value approximately beyond $M = 50$ packets. Thus, we can say that the buffer size at RS need not be greater than $M = 50$ for the system. Similarly, for staggered ARQ, the queue length saturates approximately at the buffer size $M = 40$ packets. Thus, we can conclude that since the average queue length is smaller in case of staggered ARQ as compared to hop-by-hop ARQ, the required buffer size is smaller.

In Fig. 5.11, we plot the delay D_b^{stg} due to full RS buffer and D_s^{stg}, the additional queueing delay in staggered ARQ, versus M, the size of the RS buffer. The queueing delay decreases with M since the probability of the buffer being full decreases. However, the additional delay D_s^{stg} increases with M because there being greater number of states (i, N_1), on entering which this delay occurs. Fig. 5.12 presents the comparison between the total queueing delay D_b^{hbh} in case of hop-by-hop and $D_b^{stg} + D_s^{stg}$ for staggered ARQ. D_b^{hbh} is greater than the D_b^{stg} because, in staggered ARQ, for $j \geq N_1$ consecutive bad states, the system cannot make a transition $(M-1, j-1)$ to (M, j) and enter a buffer full state. Thus, the number of states on entering which, a queueing delay occurs is smaller in case of staggered ARQ. In Fig. 5.12, we observe that for small values of M, the total queueing delay is smaller for staggered ARQ than hop-by-hop ARQ. However as M increases, the queueing delay of staggered ARQ becomes greater than hop-by-hop ARQ because both D_b^{hbh} and D_b^{stg} decrease, and D_s^{stg} becomes dominant in $D_b^{stg} + D_s^{stg}$.

Fig. 5.13 and Fig. 5.14 present comparative plots of the total packet delay T_d for

the hop-by-hop, advanced and staggered ARQ protocols. The packet delay in advanced ARQ is clearly higher than hop-by-hop ARQ and staggered ARQ because of the signalling overhead of forwarding every access link ACK/NACK to the BS. The T_d for staggered ARQ is smaller than hop-by-hop ARQ, because of a smaller queueing delay at RS due to smaller average queue length q_{avg}. Thus, we can conclude that staggered ARQ reduces packet loss during handover. Although it causes an additional queueing delay at the BS, there is a reduction in the total packet delay as compared to hop-by-hop ARQ.

5.7 Conclusions

In this chapter, we have analyzed the packet loss due to handover and packet delay in traditional multi-hop ARQ protocols - hop-by-hop and end-to-end ARQ. In particular, the packet loss can be very high in hop-by-hop ARQ because the BS is not aware of ARQ state on the access link. We have performed a theoretical analysis to determine this packet loss in terms of the average queue length at RS, and the handover probability. We have then proposed two new ARQ protocols Advanced ARQ and staggered ARQ and demonstrated the reduction in the packet loss during handover at the cost of additional signalling overhead and queueing delay respectively. The results presented in this chapter can be used to design the size of the buffer at the RS.

Future work involves performing system-level simulations to justify the channel and handover model proposed in this work. We have assumed a Markov chain model for the access channel, where the channel can be in either good or bad state. We assume that the relay channel is i.i.d. This is a reasonable assumption since the BS and RS are stationary and the relay link mostly has strong channel state. The analysis can be improved removing this assumption and considering a more practical Markov chain model for the relay channel as well. Another possible research direction is to extend this analysis to Go-back-N ARQ instead of the stop-and-wait protocol considered in this work.

Chapter 6

Conclusions and Future Work

Introduction of relay stations (RSs) in cellular networks helps improve the system capacity and coverage area. Relays have been studied extensively for ad-hoc wireless networks, but the algorithms developed cannot be directly applied to cellular networks. In this thesis, we address this challenge and design new architectures and protocols for relay-assisted cellular networks. We have analyzed three main issues - (i) RS placement for coverage extension, (ii) capacity improvement due to RSs and, (iii) the design of ARQ protocols to reduce packet loss during handover

In Chapter 3, we have analyzed optimal RS placement for the extension of coverage radius of the cell. A novel probabilistic definition of cellular coverage has been used to determine the optimal RS positions by taking shadowing and inter-cell interference into account. This analysis has considered fixed RSs placed in a symmetrical ring. A future research direction is to extend this work to self-organizing RSs, by considering the issue of placement of a new RS to remove coverage holes, given the location of existing RSs, and a propagation loss profile of the cell.

In Chapter 4, we have determined the downlink Erlang capacity of cellular OFDMA. We have used a novel approach of dividing incoming calls into service classes based on their subcarrier requirement, to compute the blocking probability of an incoming call. We have drawn an interesting analogy of the cellular OFDMA with a stochastic knapsack and applied techniques used to solve the knapsack problem to simplify the analysis of blocking probability. We have extended this idea to relay-assisted cellular system and demonstrate the capacity improvement achieved by the introduction of RSs. We have also computed the optimal RS positions and BS-RS subcarrier distribution ratio for which the capacity

improvement is maximum. The future work to be done is to evaluate various subcarrier allocation schemes based on the Erlang capacity as the performance metric. Also, this work can be extended to self-organizing RSs, which are placed at random locations in the cell as opposed to the fixed ring architecture we have considered.

In Chapter 5, we have demonstrated that heavy packet loss during handover may occur in the traditional hop-by-hop ARQ protocol. We have presented a new channel and handover model which has been used to quantify this packet loss. We have proposed modifications to hop-by-hop ARQ which reduce the packet loss during handover. Queueing and transmission delay analysis has also been performed to show that the proposed protocol gives better performance at the cost of a negligible increase in total packet delay. Our analysis assumes the stop-and-wait retransmission mechanism, and a simple two state channel model. A future research direction is to extend the analysis to Go-back-ARQ mechanism, and also consider a more realistic channel model, which captures the properties of the wireless channel more closely.

Finally, we point out some open research problems that have not been considered in this thesis. One of the most important problems for future investigation is the design of scheduling algorithm with delay constraints for a relay-assisted cellular network. Towards this, the idea of an indexing scheduler has been suggested in Chapter 2. A plethora of new research problems as described in Chapter 2 have arisen with the development of self-organizing RSs for cellular networks. We have identified the problem of intelligent subcarrier allocation in which, instead of requesting subcarrier assignment from the BS, the RSs perform neighborhood sensing and choose the subcarriers with minimum interference. Another problem is to develop an autonomous power control algorithms for user-deployed self-organizing RSs of minimizing interference to neighbors while covering the maximum possible area.

Bibliography

[1] IEEE 802.16 Broadband Wireless Access Working Group, "System Description Document for the P802.16m Advanced Air Interface," Sept. 2009.

[2] IEEE 802.16 Broadband Wireless Access Working Group, "Amendment working document for Air Interface for Fixed and Mobile Broadband Wireless Access Systems," June 2009.

[3] T. Beniero, S. Redana, J. Hmlinen, and B. Raaf, "Effect of Relaying on Coverage in 3GPP LTE-Advanced," *IEEE Vehicular Technology Conference*, vol. 53, pp. 1–5, Apr. 2009.

[4] S. Peters, A. Panah, K. Truong, and R. Heath, "Relay Architectures for 3GPP LTE-Advanced," *EURASIP Journal on Wireless Communications and Networking*, May 2009.

[5] K. Liu, A. Sadek, W. Su, and A. Kwasinski, *Cooperative Communications and Networking.* Cambridge University Press, 2009.

[6] Y. Yang, H. Hu, J. Xu and G. Mao, "Relay Technologies for WiMAX and LTE-Advanced Mobile Systems," in *IEEE Communications Magazine*, vol. 47, pp. 100 – 105, Oct. 2009.

[7] J. Tang, B. Hao, and A. Sen, "Relay node placement in large scale wireless sensor networks," *Computer Communications*, vol. 29, no. 4, pp. 490–501, 2006.

[8] H. Liu,P. Wan and X. Jia, "On optimal placement of relay nodes for reliable connectivity in wireless sensor networks," *Journal of Combinatorial Optimization*, vol. 11, pp. 249–260, Mar. 2006.

[9] B. Lin, P. Ho, L. Xie, and X. Shen, "Optimal relay station placement in IEEE 802.16j networks," in *International Conference on Wireless Communications and Mobile Computing*, pp. 25–30, 2007.

[10] S. Meko and P. Chaporkar, "Channel partitioning and relay placement in multi-hop cellular networks," in *International Conference on Symposium on Wireless Communication Systems*, pp. 66–70, 2009.

[11] B. Lin, P. Ho, L. Xie, and X. Shen, "Relay Station Placement in IEEE 802.16j Dual-Relay MMR Networks," in *IEEE International Conference on Communications*, pp. 3437–3441, May 2008.

[12] H. Wei, S. Ganguly, R. Izmailov, "Adhoc relay network planning for improving cellular data coverage," in *IEEE International Symposium on Personal, Indoor, and Mobile Radio Communications*, pp. 769–773, Sept. 2004.

[13] R. Steele, C. Lee and P. Gould, *GSM, cdmaOne and 3G Systems*. John Wiley and sons, 2001.

[14] A. Viterbi and A. Viterbi, "Erlang capacity of a power controlled CDMA system," *IEEE Journal on Selected Areas in Communications*, vol. 11, pp. 892–900, Aug 1993.

[15] K. Gilhousen, I. Jacobs, R. Padovani, A. Viterbi, L. Weaver and C. Wheatley, "On the capacity of a cellular CDMA system," *IEEE Transactions on Vehicular Technology*, vol. 40, pp. 303–312, May 1991.

[16] K. Kim and I. Koo, *CDMA Systems Capacity Engineering*. Artech House MA Inc., 2005.

[17] P. Brill and L. Green, "Queues in which customers receive simulataneous service from a random number of servers: a system point approach," *Management Science*, vol. 30, pp. 51–68, Jan 1984.

[18] B. Zhang, R. Iyer and K. Kiasaleh, "Reverse link Erlang capacity of OFDMA wireless systems with adaptive resource allocation," in *IEEE Wireless Communications and Networking Conference*, vol. 4, April 2006.

[19] H. Wang, C. Xiong, and V. Iversen, "Uplink Capacity of Multi-class IEEE 802.16j Relay Networks with Adaptive Modulation and Coding," *IEEE International Conference on Communications*, pp. 1–6, Jun 2009.

[20] C. Sunghyun, E. Jang, J. Cioffi, "Handover in multihop cellular networks," in *IEEE Communications Magazine*, vol. 47, pp. 64 – 73, July 2009.

[21] M. Lott, "ARQ for Multi-hop Networks," in *IEEE Vehicular Technology Conference*, vol. 3, pp. 1708–1712, Sept. 2005.

[22] S. Jeon, K. Han, K. Suh and D. Cho, "An Efficient ARQ mechanism in Multi-hop Relay Systems on IEEE 802.16 OFDMA," in *IEEE Vehicular Technology Conference*, pp. 1649–1653, Sept. 2007.

[23] S. Jeon, K. Han, K. Suh and D. Cho, "Modelling and Analysis of ARQ Mechanisms for Wireless Multi-hop Relay System," *IEEE Vehicular Technology Conference*, pp. 2436–2440, May 2008.

[24] J. Kim and D. Cho, "Improving TCP/IP Performance over Wireless Networks," in *IEEE Vehicular Technology Conference*, pp. 1–5, Apr. 2009.

[25] J. Kim and D. Cho, "Pre-buffering Scheme for Seamless Relay Handover in Relay Based Cellular Systems," in *IEEE Vehicular Technology Conference*, pp. 1–5, Apr. 2009.

[26] E. Yeh, R. Berry, "Throughput Optimal Control of Cooperative Relay Networks," *IEEE Symposium on Information Theory*, vol. 53, pp. 3827–3833, Oct. 2007.

[27] E. Yeh and R. Berry, "Throughput optimal control of wireless networks with two-hop cooperative relaying," *IEEE Symposium on Information Theory*, pp. 351–355, June 2007.

[28] S. Kittipiyakul and T. Javidi, "Relay Scheduling and Cooperative Diversity for Delay-Sensitive and Bursty Traffic," *Annual Allerton Conference on Communication, Control, and Computing*, Sept. 2007.

[29] H. Wang, "Cooperative Transmission in Wireless Networks with Delay Constraints," *IEEE Wireless Communications and Networking Conference*, vol. 3, pp. 1933 – 1938, Mar. 2004.

[30] I. Krikidis and J. Belfiore, "Scheduling for Amplify-and-Forward Cooperative Networks," *IEEE Transactions on Vehicular Technology*, vol. 56, Nov. 2007.

[31] H. Vishwanathan, S. Mukherjee, "Performance of Wireless Networks with Relays and Centralized Scheduling," *IEEE transactions on Wireless Communications*, vol. 4, Sept. 2005.

[32] Woo-Geun Ahn and Hyung-Myung Kim, "Proportional fair scheduling in relay enhanced cellular OFDMA systems," in *IEEE International Symposium on Personal, Indoor, and Mobile Radio Communications*, pp. 1–4, Sept. 2008.

[33] N. Salodkar, "Online Algorithms for Delay Constrained Scheduling over a Fading Channel," May 2008. PhD Thesis, Indian Institute of Technology, Bombay.

[34] H. Maral, "Downlink Erlang capacity of cellular OFDMA," 2010. Dual Degree Thesis, Indian Institute of Technology, Bombay.

[35] K. Ross, *Multiservice Loss Models for Broadband Telecommunication Networks.* Springer-Verlag New York, Inc., 1995.

[36] B. Srinadh, "Performace Analysis and Optimization of Protocols in Wireless Networks," Apr. 2010. B.Tech Thesis, Indian Institute of Technology, Bombay.